Kinematic interaction between stratigraphically discrete salt layers; the structural evolution of the Corrib gas field, offshore NW Ireland

Conor O'Sullivan[1,2], Conrad Childs[1,2]

[1] Irish Centre for Research in Applied Geoscience (iCRAG), School of Earth Sciences, University College Dublin, Belfield, Dublin 4, Ireland

[2] Fault Analysis Group, School of Earth Sciences, University College Dublin, Belfield, Dublin 4, Ireland

Corresponding author email: conor.osullivan@icrag-centre.org

Abstract

The kinematic interaction of thin salt layers during basin evolution has received little attention to date, despite there being several basins which contain multiple thin salt layers across NW Europe. This study utilises high-quality 3D seismic reflection data coupled with borehole data to investigate the evolution of the structure containing the Corrib gas field which is composed of two distinct salt structures. Located in the Slyne Basin offshore NW Ireland, the structure consists of a NE-SW oriented Permian salt pillow which folds the overlying Mesozoic stratigraphy. Upper Triassic salt acts as a second mechanical detachment and forms an elongate salt roller parallel to the crest of the Permian salt pillow. The Upper Triassic salt roller forms the footwall of a delamination fault which downthrows the anticlinal crest of the folded Jurassic section to the SE. The Permian salt pillow began rising during the Late Triassic and Early Jurassic driven by low-strain regional extension. During the main phase of rifting, a combination of basement tilting, gravity gliding, and salt welding resulted in a steep increase in the amplitude of the Permian salt pillow. The relief on the salt-cored fold resulted in gravity gliding on the Triassic salt, forming the parallel salt roller and delamination fault. The throw distribution on the delamination fault is driven by the combined mechanisms of gravity sliding on the Triassic salt and by inflation of Triassic salt in the footwall of the fault. The delamination fault is reactivated post-rift, suggesting modification of the Permian and Triassic salt structures. This study improves the understanding of the kinematic interaction of thin salt layers during syn-rift and post-rift deformation, with implications for hydrocarbon exploration on the Irish Atlantic margin and further afield.

Acknowledgements

This research is funded in part by a research grant from Science Foundation Ireland (SFI) under Grant Number 13/RC/2092 and is co-funded under the European Regional Development Fund, and by the Petroleum Infrastructure Programme (PIP) and its member companies. The authors would like to thank the Petroleum Affairs Division (PAD) of the Department of Communications, Climate Action and Environment (DCCAE), Ireland, for providing access to released well and seismic reflection datasets. Shell Exploration & Production Ireland Ltd. are thanked for providing access to reprocessed volumes of the 1997 Corrib seismic. Europa Oil & Gas are thanked for providing access to the Inishkea 2018 reprocessed seismic volume and allowing a section from the volume to be shown. The authors thank Schlumberger for providing academic licenses of Petrel to University College Dublin. The authors also thank Petroleum Experts for providing academic licenses of Move to University College Dublin.

Introduction

The presence of salt layers in the stratigraphy of a basin influences structural style both by mechanically detaching sub- and supra-salt stratigraphy during extension or compression, and by halokinesis to form salt pillows and diapirs (Jackson & Talbot, 1991; Stewart et al., 1996; Withjack & Callaway, 2000; Hudec & Jackson, 2007; Duffy et al., 2013). As salt moves from its original stratigraphic position it can also form allochthonous salt structures such as pinched diapirs and canopies. Where large salt canopies develop, they will act as a second layer of mechanical detachment and different structures can form above and below these allochthonous salt bodies. This also opens the possibility of kinematic interaction between primary and secondary halokinetic structures in the autochthonous and allochthonous salt layers (Volozh et al., 2003; Jackson et al., 2010; Dooley et al., 2013; Dooley et al., 2018). The resulting wide variety of salt-related structures has been observed and investigated in several salt-prone basins around the world, including offshore Iberia (Wilson et al., 1989; Ferrer et al., 2012; Ramos et al., 2017), the Gulf of Mexico (Peel et al., 1995; Dooley et al., 2013), offshore Morocco (Tari & Jabour, 2013) and on the Canadian Atlantic margin (Deptuck & Kendell, 2017).

There are comparatively few studies of the interaction between multiple autochthonous salt layers. In the Persian Gulf, Cambrian and Cenozoic salt layers, separated by several kilometres of intervening section, interact with one another and allochthonous bodies of the older salt layer influence both the distribution and halokinetic structures formed in the younger salt layer (Snidero et al., 2020; Hassanpour et al., 2021). Little study has been carried out on the evolution of structures in basins where multiple, relatively thin (typically less than a few 100s of metres) autochthonous layers of salt are present despite the prevalence of this stratigraphic configuration in several basins across NW Europe (Stewart et al., 1996; McKie, 2017; Hansen et al., 2020). The Slyne Basin offshore NW Ireland is an ideal natural laboratory to observe the evolution of structures in a basin with multiple thin salt layers (Fig. 1). Two main salt bodies have been proven in this basin, the Upper Permian Zechstein Group and the Upper Triassic Uilleann Halite Member (Fig. 2) and have both been active during the multiphase evolution of the basin from the break-up of Pangea during the Permian through to the opening of the North Atlantic during the Eocene (Dancer et al., 1999; Štolfová & Shannon, 2009; Stoker et al., 2017; Merlin Energy Resources Consortium, 2020; O'Sullivan et al., 2021). Permian salt pillows and rollers have been recorded throughout the Slyne Basin, while observations of Triassic salt walls and salt rollers are largely confined to the Northern Slyne Sub-basin (O'Sullivan et al., 2021). The best studied structure in the area where both salt layers are present is the anticline hosting the Corrib gas field in the Northern Slyne Sub-basin; the gas

field contains circa 1 Tcf of gas and is one of Ireland's main indigenous sources of energy (Dancer et al., 2005). Schematic models of the evolution of the structure have been presented previously (Corcoran & Mecklenburgh, 2005; Dancer et al., 2005); subsequent acquisition of high-quality seismic data and the drilling of additional wells provides the impetus for a reassessment of the structural evolution of the Corrib gas field and the interaction between the stratigraphically discrete layers of salt that formed the structural closure.

The results of this reassessment of the Corrib and adjacent structures has implications for the evolution of structural traps in other rift basins which contain multiple relatively thin layers of salt throughout their stratigraphy, such as those on the Irish Atlantic margin and across NW Europe.

Geological Setting – The Slyne Basin

The Slyne Basin is a narrow, elongate rift basin located on the Irish Atlantic margin offshore north-western Ireland (Fig. 1). The basin is 200 km long and varies between 20-60 km in width, trending broadly NNE-SSW. The Irish Mainland Shelf bounds the Slyne Basin to the east, while the Rockall Basin and Porcupine High form the western boundary. The Slyne Basin is connected to the contiguous Erris Basin to the north, which is downthrown relative to Slyne Basin across a large fault, while a narrow basement high separates the Slyne Basin from the Porcupine Basin to the southwest (Chapman et al., 1999; O'Sullivan et al., 2021). The Slyne Basin is divided into three sub-basins which are asymmetric half-grabens or grabens (Trueblood & Morton, 1991). The asymmetry of these sub-basins varies along-strike, with polarity changing across areas of structural complexity linked to underlying Caledonian structural lineaments (Trueblood & Morton, 1991; Chapman et al., 1999; Dancer et al., 1999). This study focuses on the Northern Slyne Sub-basin.

Structural Evolution

The Slyne Basin is the product of a multiphase structural evolution stretching from the Late Permian to the mid Cenozoic (Shannon, 1991; Dancer et al., 1999; Doré et al., 1999). Rifting began in the Late Permian associated with the breakup of Pangea, followed by a period of tectonic quiescence during the Triassic. A second phase of extension began during the Early Jurassic alongside a regional marine transgression, with extension continuing into the Middle Jurassic. Regional uplift and erosion occurred during the late Middle Jurassic (Merlin Energy Resources Consortium, 2020; O'Sullivan et al., 2021), before the third phase of Late Jurassic rifting began (Naylor & Shannon, 2005). Rifting ceased at the end of the Jurassic and the region experienced kilometre-scale uplift and erosion during the Early Cretaceous, creating a

distinct regional unconformity (Dancer et al., 1999; Corcoran & Mecklenburgh, 2005). The basin experienced minor extensional forces during the Cretaceous, related to rifting in the neighbouring Rockall Basin, before a second period of uplift created a second regional unconformity during the early Cenozoic (Chapman et al., 1999; Dancer et al., 1999; Corcoran & Mecklenburgh, 2005). The entire Irish Atlantic margin experienced significant magmatism related to the development of the North Atlantic Igneous Province during the Paleocene and Eocene (Corcoran & Mecklenburgh, 2005; Meyer et al., 2007; Magee et al., 2014), which manifested in the Slyne Basin as several sills that intrude throughout the basin the occurrence of extensive basaltic lava flows in the Northern and Southern Slyne sub-basins (Fig. 1 & 2).

Stratigraphic Framework

The pre-Permian sedimentary fill of the Slyne Basin consists of a Pennsylvanian sequence of sandstones and mudstones with interbedded coal horizons and a Mississippian sequence of mudstones, sandstones and limestones (Fig. 2) underlain by Silurian metasediments (Tate & Dobson, 1989; Merlin Energy Resources Consortium, 2020). The Permian section consists of a sequence of mobile salt composed predominately of halite, which changes towards the basin margins to a section dominated by clastic and carbonate lithologies (O'Sullivan et al., 2021). This Permian section is a lateral equivalent to the Zechstein Group of NW Europe. The overlying Lower Triassic Corrib Sandstone Formation consists of a near isopachous sequence (c. 330 m) of fluvial sandstones interbedded with thin layers of red mudstones (Dancer et al., 2005). These sandstones are overlain by an Upper Triassic section composed of red mudstones with thin interbeds of sandstone and siltstones belonging to the Currach Formation (Dancer et al., 1999). In the Northern Slyne Sub-basin a second layer of mobile halite is present towards the base of the Upper Triassic section, termed the Uilleann Halite Member (Merlin Energy Resources Consortium, 2020; O'Sullivan et al., 2021).

The Lower and Middle Jurassic sections in the Slyne Basin belong to the Lias and Kite groups respectively and are dominated by marine mudstones interbedded with sandstones, carbonates and thin layers of anhydrite (Trueblood & Morton, 1991; Dancer et al., 1999; Merlin Energy Resources Consortium, 2020). The overlying Upper Jurassic section is composed of several kilometres of fluvio-estuarine mudstones and sandstones belonging to the Minard Formation, which grade upwards to marine mudstones of the Sybil and Dawros formations. A major regional unconformity separates the Upper Jurassic section from the underlying Lower and Middle Jurassic section, with this unconformity removing the Middle Jurassic and the upper part of the Lower Jurassic section from the basin margins, with a more complete stratigraphic section preserved towards the centre of the basin (Dancer et al., 1999).

A distinct angular unconformity separates the Jurassic section from the Cretaceous and Cenozoic post-rift sections (Fig. 2). The Lower Cretaceous is composed of glauconitic sandstones overlain by Upper Cretaceous limestones. In the Northern Slyne Sub-basin, extensive Eocene-aged basaltic lava flows infill the karstified surface of the Upper Cretaceous limestones, which are in turn overlain by an attenuated, poorly consolidated sequence of Miocene to Recent mudstones and sandstones.

Dataset & Methodology

Dataset

This study focuses on two borehole-constrained 3D seismic reflection volumes from the Northern Slyne Sub-basin. The first is the EN3D97-REPRO, which is a subset of the larger E97IE11 3D survey acquired in 1997 which covers 660 km^2 of the Northern Slyne Sub-basin (Fig. 1). This volume was reprocessed in 2012 and provides a marked improvement in data quality over a 480 km^2 area directly overlying the Corrib gas field (Fig. 3). The second seismic volume is the 13SH3D volume, an ocean-bottom cable survey acquired between 2012 and 2013, covering 247 km^2 directly above the Corrib gas field (Fig. 1) which provides the clearest image of the Lower Triassic reservoir section (Shannon, 2018). Additional 3D seismic volumes and a single 2D seismic line to the east of Corrib (Fig. 1) were used to provide regional context across the Northern Slyne sub-basin.

The Permian and Triassic section is encountered between 2200 to 5000 mMDBRT (c. 1500-3500 ms TWTT) across most of the study area. Low frequencies of 10-15 Hz at this depth along with high velocities of 4000-5000 ms^{-1} gives a seismic resolution of 70-125 m (one-quarter wavelength sensu Brown, 2011). Seismic data quality in the Northern Slyne Sub-basin suffers due to the near-seabed geology, consisting of Eocene-aged Druid Formation basaltic lava underlain by Cretaceous-aged limestone of the Chalk Group. These features create strong multiple energy and degrade the seismic image throughout the study area (Dancer & Pillar, 2001). Seismic sections are presented in European polarity (Brown, 2001), where a positive downwards increase in acoustic impedance corresponds to a positive (red) reflection event and a decrease corresponds to a negative (blue) reflection event. All sections are vertically exaggerated by a factor of three (Fig. 3) and ball-ends are used to highlight where a fault terminates within a certain stratigraphic package, while faults without ball-ends are truncated by a younger unconformity.

The seismic database is integrated with data from all exploration, appraisal and production wells in the Northern Slyne Sub-basin. To date, five exploration wells have been drilled in the

Northern Slyne Sub-basin (18/20-1, 18/20-7, 18/25-2, 19/8-1 and 19/11-1A) along with seven appraisal and production wells from the Corrib gas field (18/20-2z, -3, -4, -5, -6z, and 18/25-1 & -3). Data from these wells includes wireline logs, cuttings descriptions, time-depth relationships, and core data from the Lower Triassic reservoir section. Additionally, a single shallow borehole from the north of the study area (19/13-sb01) includes core data from the Cenozoic section, providing greater insight into the near-seabed geology in the Northern Slyne Sub-basin. Formation tops were constrained using the most recent biostratigraphic data from the updated stratigraphic framework for offshore Ireland (Merlin Energy Resources Consortium, 2020) and these were tied to the seismic dataset using time-depth relationships in the form of checkshots.

Methodology

Five key seismic horizons were mapped across the study area (top Lower Triassic, top Upper Triassic, base Upper Jurassic, base Cretaceous and base Cenozoic) to create structure and thickness maps (in ms TWTT). The top Lower Triassic represents the top of the main reservoir unit in the study area. Because the reservoir interval is isopachous (c. 330 m thick), its base is also a proxy for the top Permian. The top Upper Triassic represents the top of the principal cap rock in the study area. The base Upper Jurassic horizon is a regional unconformity and marks the boundary between sediments deposited in the first (Early-Middle Jurassic) and second (Late Jurassic) syn-rift phases in the Slyne Basin. The base Cretaceous is a regional angular unconformity marking the cessation of rifting in the Slyne Basin and the first stage of post-rift deposition. The base Cenozoic is another regional unconformity and represents the onset of thermal subsidence in the neighbouring Rockall Basin to the NW. Time-thickness maps were generated between mapped horizons to analyse thickness variations in syn- and post-rift sections and to provide qualitative constraints on the evolution of faults and halokinetic structures.

To analyse brittle deformation in the Jurassic supra-salt section and its relationship to the evolution of halokinetic structures throw-distance plots were created for the base Upper Jurassic Unconformity, the Base Cretaceous Unconformity and the top of the Druid Formation (Early Eocene) on the main delamination fault located above the Corrib anticline. The throw-distance plots were then overlain above strike-sections of concordant Triassic and Permian salt structures to assess spatial correlation and kinematic coherence between the discrete halokinetic structures and their overburden (Walsh & Watterson, 1991; Childs et al., 1993).

To carry out 2D structural restoration, a velocity model was created to convert seismic sections from the time to depth domain. The layer model consisted of intervals defined by the seabed,

base Druid Formation (Base-Cenozoic Unconformity), base Cromer Knoll Group (Base-Cretaceous Unconformity), base Minard Formation (Base Upper Jurassic Unconformity), top Currach Formation (Upper Triassic), top Corrib Sandstone Formation (Lower Triassic) and top Zechstein Group (Upper Permian). An initial interval velocity and k-factor (the change in interval velocity with depth) were calculated for each interval using data from wells within the EN3D97-REPRO seismic volume.

Structural restoration was carried out on a NW-SE oriented representative seismic cross-section through the Corrib gas field taken from the EN3D97-REPRO seismic volume. Restoration was carried out using a combination of 2D decompaction and move-on-fault algorithms for the Cenozoic, Cretaceous and Upper Jurassic sections, following established methodologies for restoration in salt-influenced basins (Rowan, 1993; Roberts et al., 1998; Rowan & Ratliff 2012; Macaulay, 2017). Estimations for missing Cretaceous and Upper Jurassic sections (100 and 1400 metres respectively) were taken from Corcoran & Mecklenburgh (2005). A combination of 2D decompaction, move-on-fault and unfolding by flexural slip (i.e. constant bed length) algorithms was used to reconstruct the Early and Middle Jurassic evolution of the Corrib structure during the early phases of halokinesis. Decompaction is performed using the Sclater & Christie (1980) function with most of the Mesozoic section being siliciclastic-dominated apart from the Late Cretaceous Chalk Group, which is carbonate-dominated. Flexural isostasy was used to compensate for sedimentary loading, using a crustal density of 2.75 g/m^3 and a crustal thickness of 30 km (O'Reilly et al., 1995; Kimbell et al., 2010). As no accurate base-salt horizon can be interpreted in the Northern Slyne sub-basin on the data available to this study, a schematic representation is included on restored sections indicating a possible sub-salt geometry, based on the interpretation of basement geometries in other parts of the Slyne Basin. The impact of igneous intrusions on the sedimentary column is another uncertainty (sensu Mark et al., 2019). While large intrusions are present throughout the stratigraphy (Fig. 3) they make up a very small proportion of the stratigraphy encountered by drilling in the study area (Merlin Energy Resources Consortium, 2020).

Results

Structural Configuration

The structure containing the Corrib gas field consists of three discrete elements which share a linked evolution (Fig. 3, 4); the Lower Triassic section is folded by a Permian salt pillow, creating a NE-SW trending anticline which is 12 km long and 5 km wide (Fig. 5). The anticline is flanked by synclines to the NW and SE, with the synclinal trough to the SE being around 300 ms TWTT deeper. A small satellite closure is present 8 km north of the Corrib fold, forming

the ‘Corrib North’ faulted anticline drilled by the 18/20-7 well (Fig. 1). Due south of the Corrib anticline is a fault-bounded basement high which was drilled by the 18/25-2 ‘Shannon’ well (Fig. 1). This high is bounded by a fault trending WNW-ESE which wraps around the high to trend NE-SW (Fig. 1).

The overlying Upper Triassic salt forms a narrow, 8 km long salt wall trending NE-SW (Fig. 5). This salt wall trends parallel to the fold axis of the underlying salt-cored fold, but is offset from the apex of the fold by 1 km to the NW. The 18/20-2z and 18/20-6z wells penetrate the salt wall at its thickest point (c. 600 ms TWTT), encountering 783 and 704 m of halite with interbedded layers of red mudstone respectively (Merlin Energy Resources Consortium, 2020). This salt decreases in thickness away from the crest of the Corrib anticline, with the Uilleann Halite Member making up only 13 m of the total 107 m of the Upper Triassic section in the 18/20-7 well (Shell, 2011).

The Upper Triassic salt wall forms a roller in the footwall of a large SE-dipping delamination fault (termed the Corrib fault in this study) which soles out in the Upper Triassic salt and trends parallel to the fold-axis of the Permian salt pillow in a NE-SW orientation (Fig. 3-5). A faulted rollover in the hanging-wall of the Corrib fault is interpreted to have formed by salt-cored folding of the Jurassic overburden by the Permian salt pillow, displaced by movement on the Corrib fault. This rollover is deformed by a series of smaller antithetic and synthetic faults which also sole out in the Uilleann Halite Member. The Corrib fault has a sigmoidal trace in map view (Fig. 5), where the north-eastern and south-western ends of the fault are oriented ENE-WSW and oblique to the NE-SW orientation of the central portion of the fault (Fig. 3). Two fault splays in the hanging wall of the Corrib fault are interpreted to represent breached relay ramps (Fig. 4, 5).

Unlike the Jurassic section, the post-rift sediments are largely undeformed, with a distinct truncation of the folded Upper Jurassic sediments at the relatively flat-lying Base-Cretaceous Unconformity (Fig. 3, 4). Both the Cretaceous and Cenozoic sections dip gently towards the NW, likely a result of post-rift thermal subsidence in the neighbouring Rockall Basin during the Cenozoic (Fig. 1) and are offset by normal movement on the Corrib fault (Fig. 3, 4). In addition to the reactivation of the Corrib fault, a series of ENE-WSE oriented faults is observed deforming the Cretaceous and Jurassic section 5 km to the SE of the Corrib structure (Fig. 5), likely related to rifting in the Rockall Basin during the Cretaceous. Faults of a similar age, magnitude and orientation have recently been identified in the Porcupine Basin to the SW of the study area (Saqab et al., 2020). The Cretaceous faults in the Corrib area appear to have been exploited by Cenozoic sills that intrude into the Upper Jurassic and Cretaceous sediments to the SE of the Corrib structure, causing doming and folding in the overlying

Cretaceous sediments (Fig. 3, 5B, 6). These sills do not deform the base of the Druid Formation lavas (dated 40-54.3 Ma, Dancer et al., 2005), with the crests of the sill-induced folds eroded by the unconformity at the base of this section, indicating the sills pre-date the extrusion of these early-mid Eocene volcanics. In addition to these sills which intrude into the Upper Jurassic section directly beneath the Base-Cretaceous Unconformity, there are several other intrusions observed in the Lower and Middle Jurassic section which may be coeval. These deeper sills are more strata concordant when compared to the saucer shape morphology of their shallower counterparts (Fig. 3).

Isochron analysis

The mapping of significant seismic horizons allows the vertical thickness of different sedimentary packages to the be calculated and displayed as isochron maps (in ms TWTT). Isochrons were generated for the Upper Triassic (Currach Formation and Uilleann Halite Member), Lower-Middle Jurassic (Penarth, Lias, and Kite groups), Upper Jurassic (Beara and Muckross groups), and Cretaceous (Cromer Knoll and Chalk groups) sections within the EN973D-REPRO seismic volume (Fig. 7).

The elongate salt wall above the Corrib anticline is clearly visible on the Upper Triassic isochron map, trending NE-SW parallel to the fold axis of the Lower Triassic salt-cored fold (Fig. 7D). The Currach Formation thickens significantly into the hanging-wall of a N-S oriented fault due east of the Corrib anticline, reaching thicknesses greater than 600 ms TWTT (Fig. 7D). As the throw on this fault is greater than the thickness of the Lower Triassic Corrib Sandstone Formation, there may be mixing of Upper Triassic and Permian salt and mudstone in the fault plane (Fig. 5, 7D). The Upper Triassic section also thickens in the syncline to the NW of the Corrib anticline (Fig. 3, 7D), suggesting that halokinesis may have begun during the Late Triassic, possibly driven by active faults in the sub-salt basement.

The Lower and Middle Jurassic sections thicken into the synclines flanking the Corrib anticline while they thin onto the crest of the fold (Fig. 7C). The sequence in the syncline to the NW is c. 250 ms TWTT thicker than in the SE syncline, suggesting asymmetry in the salt-cored fold during the Early and Middle Jurassic. The dislocation of the axis of the thickened Lower and Middle Jurassic section relative to the Triassic depocenter mentioned above suggests that halokinesis of the Triassic salt may have begun during this time (Fig. 3). The NW-SE oriented fault south of Corrib was active during the Early and Middle Jurassic, and a significantly thinner section of Lower and Middle Jurassic sediments are observed on the footwall of this fault block (Fig. 7C).

The polarity of the depocenters changed during the Late Jurassic, with a significantly thicker Upper Jurassic section present in the syncline to the SE (Fig. 7B). During this time there was significant regional extension and movement on the basin-bounding faults to the SE of the Corrib structure (Fig. 1D). Comparison with seismic sections shows a broad eastward fanning of reflectors (Fig. 3) towards the basin-bounding fault system east of Corrib (Fig. 1) while there is no clear indication of growth sequences in the hanging-wall of the Corrib fault (Fig. 3). The inconsistency between the thickness changes recorded in the Upper Jurassic isochron (Fig. 7B) and reflector geometries on seismic sections can be explained by early Upper Jurassic, Beara Group deposition being primarily controlled by movement on the basin-bounding fault system to the east of Corrib, while growth of the Permian salt pillow occurred at a later stage of Late Jurassic rifting, with evidence of this growth on the seismic data lost due to post-rift erosion.

There is evidence of fault activity during both the Cretaceous and Cenozoic, with the Cretaceous Cromer Knoll and Chalk groups thickening into the hanging wall of the Corrib fault, as well as the ENE-WSE faults which formed during this time (Fig. 3, 4, 7A). The impact of the Cenozoic sills is also observed on the Cretaceous isopach, with erosion above the SE syncline where several sills intrude into the Upper Jurassic section directly beneath the Base Cretaceous Unconformity (Fig. 6, 7A).

Fault analysis

The Corrib fault is a SE dipping listric fault which soles out in the Upper Triassic Uilleann Halite Member and has a total length of 24 kilometres (Fig. 5, 8). The greatest throws on the fault are almost 450 ms TWTT and occur at the base of the Upper Jurassic section (Fig 8A) The cumulative throw of the fault and two large hanging wall splays is greater than 350 ms TWTT for a 10-kilometre-long section at the centre of the fault directly overlying both the Upper Triassic and Permian salt structures (Fig. 8A, B). The throw of the primary Corrib fault decreases sharply to the SW from over 300 ms TWTT to under 50 ms TWTT over a kilometre, with much of this strain being transferred to a breached relay zone (R1) and nearby faults (S1 and S2; Fig. 8 A, E). There is a more gradual decrease in throw to the NE, where throw decreases from 350 ms TWTT to 50 ms TWTT over four kilometres (Fig. 8A). The throw distribution on the fault broadly correlates with the along-strike elevation at the Top Triassic horizon (compare the cumulative throw curve in Fig. 8A with the Top Currach Formation elevation in Fig. 8B) demonstrating a kinematic connection between fault offset and the movement of the salt layers that has generated this topography.

Within the Jurassic section only the Base Upper Jurassic Unconformity can be used to construct a throw profile, primarily because it is difficult to define Lower and Middle Jurassic hanging wall cut-offs due to the listric fault geometry and the lack of continuous reflectors in the Upper Jurassic section. Cross-sections through the fault and local well developed Lower to Middle Jurassic reflectors (e.g. Fig. 3, 8E-G) do not indicate any appreciable growth of the Corrib fault in this interval and the Lower and Middle Jurassic thickness variations adjacent to the fault are related to salt movement or later structural thinning. The throw profile constructed at the Base Upper Jurassic Unconformity is therefore thought to record most of the Jurassic throw on this fault. Throw profiles with throw maxima of 50 ms TWTT and 150 ms TWTT (Fig. 8A) for the Druid Formation and Base Cretaceous Unconformity, respectively, record post-rift resolvable reactivation along up to 20 km of the fault; sub resolution post-rift movement may have occurred along its entire length. Comparison between the throw profiles for the different offset horizons (Fig. 8A) demonstrates that most of the fault throw accumulated before the deposition of the preserved Cretaceous section and simple backstripping of the post-rift fault throw (Chapman & Meneilly, 1991; Petersen et al., 1992; Childs et al., 1993) indicates that the cumulative throw on the Corrib fault towards the end of the Late Jurassic i.e. before post-rift tectonic activity, was a maximum of 300-350 ms TWTT (Fig. 8C).

The jagged trace of the Corrib fault and three significant splays in the hanging wall of the fault (Fig. 8D) indicate that the fault developed through linkage of a series of left-stepping faults where the splays are the locations of earlier relay ramps that have been breached. Approximate timing of the breaching of these relay zones can be estimated from the seismic data and the fault throw profiles. The seismic data indicate that the hanging wall splays terminate upwards within the Upper Jurassic section (Fig 8E-G) suggesting they became inactive during this interval. The throw on the splays at the branchpoint with the throughgoing fault can also give an indication of the throw at which the relay ramps were breached, and fault segments became connected. For both relay zones R1 and R2 the throw on the splay where it intersects the main Corrib fault is 150 ms TWTT (Fig. 8A) indicating the throw on the fault when the relay zones were breached occurred when the throw on the Corrib fault was 150 ms TWTT and more than half of its throw at the end of the Jurassic. The pattern of left-stepping faults continues along-strike both north and south of the Corrib fault, but at these locations the fault throw is insufficient to cause breaching of the 1 to 3 km wide relay zones (Fig. 8).

The initiation of the Corrib fault as a series of left-stepping faults requires explanation. If the fault formed in response to the rise of the Permian or Triassic salt structures alone then the faults would be expected for form broadly parallel to their axes (i.e. oriented NE-SW). However, the obliquity of the initial fault segments, which are oriented ENE-WSW, suggests

that extensional stresses unrelated to these structures played a significantly role in fault initiation. These extensional stresses could be of direct tectonic origin. At the time of fault initiation (during the Early to Middle Jurassic), the Jurassic section would have been decoupled from the basement by both the Upper Triassic and Permian salt layers so that the orientation of these faults may be a direct indicator for the Early Jurassic extension direction. Alternatively they could be of gravitation origin resulting from the SE tilting towards the active basin-bounding fault. The second of these options is favoured as the basin opening direction is thought to be approximately perpendicular to the basin axis. It is not possible to determine from the data whether the en echelon fault array initiated during the relatively minor Early to Middle Jurassic or the main Late Jurassic phase of rifting.

Although tectonically induced stresses, direct or indirect, are likely to have played a significant role in the initiation of the Corrib fault, the main driver for the accumulation of throw is salt movement as is apparent from the strong correlation between horizon elevation and fault throw (Fig. 8 A, B). The Upper Triassic and Permian salt layers provide two potential mechanisms for driving fault movement. The first mechanism is gravity sliding on the flank of the rising Permian salt pillow, where the Upper Triassic salt acts as a décollement accommodating the downthrow of the hanging wall of the fault. The second mechanism is the relative uplift of the footwall by growth of the Upper Triassic salt wall, which is supported by the seismic cross-sections (Fig. 1, 3) and the Late Triassic isopach map (Fig. 7D). By comparing the topography along the length of the fault with the fault throw distribution we can place some constraints on the relative magnitudes of these two drivers.

The topography along a profile at the Top Currach Formation has two components: the topography of the Permian salt pillow and the irregular thickness of the Upper Triassic salt wall. The intervening isopachous Lower Triassic makes no contribution to topographic variation. Were all throw on the fault due to inflation in its footwall, there should be a one-to-one correspondence between the topographic contribution from the Upper Triassic salt and the throw. However, the topographic contribution of the Upper Triassic salt is lower than the total throw on the Corrib fault along its entire length by between 100 and 200 ms TWTT (Fig. 8C). The excess throw is considered to be driven predominantly by sliding on the flank of the Permian salt pillow although there is also likely to be some relatively minor tectonic contribution. The Triassic salt thickness and associated contribution to throw from the salt wall is greatest at the centre of the Corrib fault, where it accounts for 300 of the 400 ms TWTT total throw (Fig. 8A-C) while north and south only 100 ms of the throw can be attributed to the salt wall. This pattern can be rationalised in terms of the respective wavelengths of the Permian and Upper Triassic salt structures; the Permian salt pillow extends beyond the Triassic salt wall both to the north and south, indicating the rise of Permian salt is the driver for fault

movement on the northern and southern ends of the fault, with a progressive decrease in amplitude of the Permian salt pillow reflected in the reduced fault throw.

A notable feature of previous interpretations of the Corrib structure was faults antithetic to the Corrib fault. These faults have been interpreted as an Early Jurassic listric fault which dipped towards the NW before the polarity of the Corrib fault changed to that observed at present (Dancer et al., 2005; Corcoran & Mecklenburgh, 2005). Modern seismic data reveals that most of these faults are not through going and are instead comprised of two discrete fault families; a lower set of faults which offset horizons within the Lower and Middle Jurassic section and generally terminate upwards in the Upper Jurassic section (Fig. 3, 8D), and a second set of primarily Late Cretaceous faults offsetting Cretaceous and Jurassic horizons before being truncated by the Base Cenozoic Unconformity (Fig. 3). Polarity reversal of the Corrib fault is also difficult to justify with the evidence presented above.

Evolution of the Corrib structure

Structural restoration was performed on a representative seismic section across the Corrib structure (Fig. 9) using the context provided by observations described above. As the pre-salt basement is not clearly imaged within the study area, a schematic basement geometry was included in each stage of the structural restoration to showcase the potential influence basement geometry had on halokinesis and structural evolution, using context from other areas of the Slyne Basin (e.g. Trueblood & Morton, 1991; Dancer et al., 1999; O'Sullivan et al., 2021).

The Early Triassic Corrib Sandstone Formation is largely isopachous throughout the Slyne Basin (Merlin Energy Resources Consortium, 2020) indicating a period of tectonic quiescence in the area. Thickening of the Currach Formation to the NW of Corrib (Fig. 3, 7D) suggests that the movement of Permian salt began during the Late Triassic, likely driven by active faulting in the sub-salt basement (Fig. 9). Evidence for Late Triassic fault activity in the Slyne Basin has not been reported previously but has been observed in other areas including the Erris, Larne and Kish Bank basins (Chapman et al., 1999; Dunford et al., 2001; Fyfe et al., 2020). The Triassic depocenter suggests this Late Triassic extension may have extended to the Slyne Basin.

A relatively isopachous section of interbedded shallow marine mudstones, sandstones and limestones were deposited in the Northern Slyne Sub-basin during the Hettangian to Sinemurian (Fig. 10). A stratigraphic break occurred towards the end of the Pliensbachian, forming a minor regional angular unconformity above the crest of the incipient salt Permian

pillow (Fig. 3, 9, 10). This was followed by the deposition of a thicker section of Toarcian and Middle Jurassic sediments in the synclines to the NW and the SE (Fig. 7C, 9, 10).

A well correlation through the three wells which penetrate a complete Lower and Middle Jurassic section within the EN3D97-REPRO seismic volume highlights both the thickening of this section in the syncline to the NW as well as the erosion and reduced section present across the crest of the salt-cored fold (Fig. 10). A circa 300 m section of the Pabay Shale Formation has been eroded at the 18/25-1 well location, while a conformable contact is observed between the Whitby Mudstone and Pabay Shale formations in both the 18/20-1 and 18/20-7 wells (Merlin Energy Resources Consortium, 2020). Additionally, a thinned section of Whitby Mudstone Formation is present on the crest of the salt-cored fold that is roughly half the thickness of the section recorded off-structure. The broadly isopachous Inagh, Meelagh and Conn formations observed across the area indicates that there was little salt movement during the Hettangian and Sinemurian (Fig. 10). The array of ENE-WSE oriented fault segments that preceded the Corrib fault likely began forming during the late Early and Middle Jurassic, driven by regional extensional stresses (Fig. 9)

A stratigraphic break occurred during the Bathonian and Callovian along with local erosion, to form the regional Base Upper Jurassic Unconformity observed throughout the Slyne Basin (Merlin Energy Resources Consortium, 2020). Regional extension during the Late Jurassic resulted in kilometre-scale movement on the faults bounding the Northern Slyne Sub-basin to the SE (Fig. 1D) which would have caused the sub-salt basement to dip towards the SE, leading to gravity sliding on the mechanically weak salt layers (Fig. 9). The polarity of the salt-cored fold would have changed as a result, with a thicker Upper Jurassic section being deposited in the syncline to the SE which is adjacent to the active basin-bounding fault (Fig. 7). Sediment loading in the immediate hanging-wall of the basin-bounding fault (i.e. the SE syncline) would have resulted in the movement of Permian salt away from the SE syncline and into the pillow, resulting in the welding of the Lower Triassic and Carboniferous basement (Fig. 9). The welding of the Triassic section to the sub-salt basement beneath the SE syncline formed a barrier to the continued south eastward gravity gliding of the section up-dip, resulting in further inflation of the Permian salt pillow (Fig. 9). As the relief of the Permian salt pillow increased along with regional extension and salt inflation, gravity gliding occurred on the Upper Triassic salt layer (Fig. 9). Outer-arc extension associated with the salt-cored fold and gravity gliding on the Upper Triassic salt led to the reactivation of Early-Middle Jurassic fault system, forming the Corrib fault through fault linkage and the breaching of relay ramps, downthrowing the axis of the folded Jurassic section to the SE (Fig. 9).

The Slyne Basin experienced kilometre-scale uplift and erosion as rifting ceased at the end of the Jurassic. Corcoran & Mecklenburgh (2005) estimate over a kilometre of the Upper Jurassic section was removed above the Corrib anticline during the Early Cretaceous, and that there may have been movement on the Corrib fault during this period of exhumation. Following this regional uplift and erosion, a relatively thin section of Cretaceous sediments was deposited across the Northern Slyne Sub-basin. The Corrib fault was reactivated during the deposition of both the Early and Late Cretaceous sections with growth strata observed in the hanging wall, while a series of shallow faults oriented NE-SW formed during the Late Cretaceous above the crest of the Jurassic rollover in the hanging wall of the Corrib fault (Fig. 3, 8). This post-rift activity on the Corrib fault was likely caused by modification of the Permian and Triassic salt structures driven by regional tectonic events such as rifting and hyperextension in the neighbouring Erris and Rockall basins to the NW (Knott et al., 1993; Chapman et al., 1999; Zeigler & Dèzes, 2006). The ENE-WSW faults located to the SE of Corrib also formed during this time (Fig. 5, 7).

A second phase of regional uplift and erosion occurred during the early Cenozoic with an estimated 50-150 metres of Late Cretaceous sediments removed above the Corrib structure (Corcoran & Mecklenburgh, 2005). Several sills intruded into the Mesozoic section throughout the Slyne Basin during the early Cenozoic; at depth these sills were concordant with the Lower and Middle Jurassic stratigraphy (Fig. 3, 8E), while those intruding into the shallow Upper Jurassic and Cretaceous section caused folding and faulting, with the crests of sill-induced folds eroded during this phase of uplift (Fig. 6). The volcanics of the Druid Formation were extruded onto this early Cenozoic unconformity across the Northern Slyne Sub-basin and appear to post-date the sill-related folding and deformation (Fig. 6). The delamination fault was reactivated for a second time during this time, with a thicker section of Druid Formation and overlying Hebrides Margin and Eilean Siar group sediments preserved in the hanging wall (Fig. 3, 4). Thermal subsidence in the hyperextended Rockall Basin occurred during this time (Chapman et al., 1999; Doré et al., 1999) and was likely the strongest driver of Cenozoic post-rift deformation, with differential subsidence occurring along the NW margin of the Slyne basin, most evident on a regional transect of the Northern Slyne Sub-basin (Fig. 1D).

Discussion

Revised structural evolution of the Corrib gas field

Previous models for the structural evolution of the Corrib structure proposed that the polarity of the Triassic salt roller and resultant delamination fault changed during the evolution of the structure (Corcoran & Mecklenburgh, 2005; Dancer et al., 2005). They have interpreted a fault

dipping to the NW prevailing during the Early and Middle Jurassic before a polarity reversal resulted in the SE dipping fault during the Late Jurassic observed at present. This is based on the interpretation of erosion and a missing section of the Lower and Middle Jurassic section on the SE flank of the Corrib structure (Corcoran & Mecklenburgh, 2005: Dancer et al., 2005). These authors interpreted the erosion as the product of a 'Base-Middle Jurassic Unconformity' and is equivalent to the unconformity observed at the base of the Whitby Mudstone Formation observed over the crest of the Corrib structure (Fig. 2, 3), dated as late Pliensbachian to early Toarcian in the revised stratigraphic framework for offshore Ireland (Merlin Energy Resources Consortium, 2020).

On modern seismic data this erosion is relatively subtle and is symmetrical, with erosion and reflector truncation observed on both the NW and SE flank of the salt cored fold (Fig. 3). The impact of this erosion is recorded in the 18/25-1 well on the crest of the Corrib anticline, where circa 300 m of the Pabay Shale Formation is absent and is overlain by a reduced Whitby Mudstone Formation relative to the stratigraphy encountered off structure (Fig. 10). Given the relatively structural immaturity (sensu Jackson & Talbot, 1991; Hudec & Jackson, 2007) of the salt structures observed in the Northern Slyne Sub-basin, the symmetrical erosion pattern is more readily associated with the less complex growth of a salt pillow (Stewart & Coward, 1995; Hudec & Jackson, 2017). The apparent offset between the axes of the Late Triassic and Early Jurassic depocenters observed in the syncline to the NW of Corrib suggests that the latter may have been the product of Triassic salt movement during the Pliensbachian and Toarcian rather than further withdrawal of Permian salt from the NW syncline. While polarity reversal of large listric faults adjacent to rising salt diapirs is observed, it is more commonly observed in structurally mature salt diapirs (Quirk & Pilcher, 2012). Nevertheless, the asymmetry and variation in thickness between the Upper Jurassic and Lower to Middle Jurassic sections observed by previous authors is confirmed in this study as a product of halokinesis.

The kinematic interaction between discrete salt layers and Corrib analogues in the Slyne Basin

The distinctive structure of the Corrib gas field formed through the combined effects of salt migration in two distinct salt layers. The throw on the Corrib fault was driven by two different but interdependent halokinetic processes, the delamination of the hanging-wall and footwall inflation. The relative importance of these mechanisms varies along the length of the Corrib structure and may also have varied through time. There are a number of Corrib-like anticlinal structures within the Northern Slyne Sub-basin (Fig. 1A). While these deform the same

stratigraphic template and have features in common with the Corrib structure, they also display a varied response to the pillowing of Permian salt.

The ‘Cong’ structure most closely resembles the Corrib gas field (Fig. 1A). It has a similar structural geometry and scale, being a 15 km long and 5 km wide fold at Lower Triassic level cored by a Permian salt pillow (Fig. 1). In common with Corrib, a listric delamination fault cuts across the anticline, offsets the Jurassic overburden and soles out in the Upper Triassic salt. Unlike Corrib the delamination fault was not active after the Middle Jurassic and terminates at the Base Upper Jurassic Unconformity despite the similarity in amplitude of these two structures. A possible explanation for the lack of Late Jurassic faulting in the Cong structure is that, unlike Corrib, there was no tectonically induced tilting during the Late Jurassic.

A second structure of similar scale is Inishkea West which lies 20 km to the west of Corrib (Fig. 1). In this case, delamination faults occur on both flanks of the Permian salt pillow, dipping away from the crest rather than cutting across it and extend upwards to the Base Cretaceous Unconformity. The fault on the western flank is much larger than those on the eastern flank, and the offset is far larger than would be expected due to gravity sliding related to the growth of the Permian salt pillow. This west dipping fault must have achieved its displacement in response to the westward tilting of the basin following its initiation on the flank of the Permian salt pillow.

Other variations in the style of deformation in the Slyne Basin can be seen by inspection of Fig. 1E. A low amplitude salt pillow, Corrib North, shows subtle Lower-Middle Jurassic thinning onto the anticlinal crest but no evidence for the formation of a delamination fault. In contrast to Corrib North, and 8 km to the NW, is a large (500 ms TWTT throw) delamination fault that soles out in the Upper Triassic salt, with thickened Upper Triassic salt in the footwall but no obvious thickening in the underlying Permian. These two structures demonstrate that the processes that drove the formation of the Corrib structure, and presumably also Cong and Inishkea West, can also occur individually.

It is tempting to consider the Corrib North, Cong, Corrib and Inishkea West structures as illustrating development stages of Permian salt pillow growth and the initiation of delamination faults during the Early-Mid Jurassic followed by Late Jurassic tectonic induced tilting leading to increased throw on the delamination faults. However, this is likely an oversimplification as the evolution of structures is influenced by multiple interacting factors including variations in primary salt thickness and welding of different salt layers.

Kinematic interaction between discrete, thin layers of salt

Several basins across NW Europe, particularly those within the Southern Permian Basin, have a similar stratigraphic configuration to the Slyne Basin and contain both Permian and Upper Triassic salt layers. These include the Sole Pit and Lower Saxony basins and the Danish Central Graben (Stewart et al., 1996; Kockel, 2003; Duffy et al., 2013). Relative to the Slyne Basin, these areas have significantly greater volumes of Permian salt while salt within the Upper Triassic is restricted to thin layers within a mudstone-dominated section. Nevertheless, analogues to the Corrib gas field are observed; the most striking of these is the Kraka salt pillow in the Danish Central Graben. This structure consists of a Permian salt pillow of similar dimensions to Corrib (8 km wide and 10 km long with an amplitude of circa 1 kilometre) which folds the overlying Mesozoic stratigraphy coupled with delamination faulting soling out in layers of Triassic salt (Duffy et al., 2013; Hansen et al., 2020). Small rollers of Triassic salt are also observed beneath the footwalls of these delamination faults (Hansen et al., 2020). The Corrib and Kraka structures differ in the manner of their later post-rift reactivation; the Corrib structure is subjected to extensional deformation associated with nearby hyperextension and thermal subsidence in the Rockall Basin, while the Kraka structure is impacted by compressional tectonics driven by the Alpine Orogeny. Nevertheless, their pre-inversion geometries are near-identical (Hansen et al., 2020 Figure 13 therein).

The variety of structures observed in the Northern Slyne Sub-basin and further afield demonstrates that while the interaction of salt layers likely follows a similar geological evolution early in their genesis, as strain values increase their evolution diverges. Where two layers of salt are present in the stratigraphy of a rift basin, the older salt typically begins to flow first, possibly before the deposition of the second layer. Salt flow and the formation of halokinetic structures in the older salt creates topography that will influence and localise the formation of secondary halokinetic structures in the younger salt layer, such as outer arc extension at the crest of a salt-cored fold. As these structures continue to evolve factors such as local salt thickness, basin geometry and post-rift deformation result in greater variation. Within the Northern Slyne Sub-basin the style of deformation is largely controlled by these considerations but also the degree of tectonic tilting with increasing tectonic strain that determines the extent to which the delamination faults are amplified.

Conclusions

Using modern, borehole-constrained 3D seismic reflection data a detailed model of the Corrib gas field offshore NW Ireland and its structural evolution has been developed. The Corrib gas field consists of three principal components:

- A relatively simple NE-SW trending salt-cored fold at the Lower Triassic stratigraphic level above an elongate pillow of Permian salt.
- An Upper Triassic salt wall trending parallel to the underlying salt-cored fold.
- A complex overburden of Jurassic syn-rift and Cretaceous and Cenozoic post-rift sediments deformed by a listric delamination fault (the Corrib fault) which dips towards the SE and soles out in the Upper Triassic salt.

The multiphase structural evolution of the Corrib gas field is a result of rifting in the Slyne Basin during the Late Triassic, Early to Middle Jurassic and Late Jurassic, followed by post-rift deformation in the Cretaceous and Cenozoic:

1. The structure initiates with movement of the Permian salt during the Late Triassic and the formation of a thickened Upper Triassic depocenter, possibly driven by faulting in the sub-salt basement before tectonic quiescence ensues during the earliest Jurassic.
2. Mild regional extension results in salt movement recommencing during the late Early Jurassic with the growth of the Permian salt pillow and initiation of an Upper Triassic salt pillow, both of which fold the overlying Jurassic sediments. This salt-cored fold is asymmetric, with a thicker depocenter forming in the syncline to the NW. An oblique array of en echelon faults forms in the Jurassic section due to regional extension.
3. The main phase of rifting occurs during the Late Jurassic with kilometre-scale movement on the faults bounding the Northern Slyne Sub-basin. Basement titling results in gravity gliding and a reversal in the asymmetry of the salt-cored fold, with a thicker depocenter developing in the syncline to the SE. A combination of up-dip gravity gliding on the Permian salt and sediment loading inflates the Permian salt pillow, which in turn results in gravity gliding on the Upper Triassic salt above the crest of the rising salt-cored fold. The pre-existing fault system in the Jurassic section is reactivated as a major listric delamination fault (the Corrib fault) through the breaching of relay ramps and segment linkage, down throwing the anticlinal crest of the Jurassic salt-cored fold towards the SE. As extension continues, Upper Triassic salt forms an inflated, elongate salt roller in the footwall of the delamination fault. The final throw distribution on the Corrib fault is a response to both gravity sliding on Upper Triassic salt driven by growth of the Permian salt pillow, and inflation of Upper Triassic salt in the footwall.
4. Following the cessation of the rifting at the end of the Jurassic, the Northern Slyne Sub-basin experiences kilometre-scale uplift and erosion. Rifting in the neighbouring Rockall Basin results in reactivation of the delamination fault and the modification of halokinetic structures.
5. Post-rift thermal subsidence in the Rockall Basin results in differential subsidence along the western margin of the Northern Slyne Sub-basin. The delamination fault is

reactivated for a second time. At the same time, sills intrude throughout the Mesozoic section in the area, followed by the extrusion of lavas across the Northern Slyne Sub-basin during the Early Eocene.

The evolution of the Corrib structure demonstrates kinematic interaction between thin salt layers. Other anticlinal features in the Northern Slyne Sub-basin also demonstrate thin-skinned deformation in the form of gravity gliding on the Upper Triassic salt, above rising Permian salt structures driven by a combination of regional tectonic forces and sedimentary loading. While demonstrating the same two-salt deformation features, the variation between these structures can largely be attributed to the magnitude of local Late Jurassic tilting.

References

Chapman, T.J., Broks, T.M., Corcoran, D. V., Duncan, L.A. & Dancer, P.N. 1999. The structural evolution of the Erris Trough, offshore northwest Ireland, and implications for hydrocarbon generation. *Petroleum Geology of Northwest Europe: Proceedings of the 5th Conference*, 455–469.

Chapman, T.J. & Meneilly, A.W. 1991. The displacement patterns associated with a reverse-reactivated, normal growth fault. *Geological Society, London, Special Publications*, **56**, 183–191, https://doi.org/10.1144/GSL.SP.1991.056.01.12.

Childs, C., Easton, S.J., Vendeville, B.C., Jackson, M.P.A., Lin, S.T., Walsh, J.J. & Watterson, J. 1993. Kinematic analysis of faults in a physical model of growth faulting above a viscous salt analogue. *Tectonophysics*, **228**, 313–329, https://doi.org/10.1016/0040-1951(93)90346-L.

Corcoran, D. V & Mecklenburgh, R. 2005. Exhumation of the Corrib Gas Field, Slyne Basin, offshore Ireland. *Petroleum Geoscience*, **11**, 239–256, https://doi.org/10.1144/1354-079304-637.

Dancer, P.N., Algar, S.T. & Wilson, I.R. 1999. Structural evolution of the Slyne Trough. *Petroleum Geology of Northwest Europe: Proceedings of the 5th Conference on the Petroleum Geology of Northwest Europe*, **1**, 445–454, https://doi.org/10.1144/0050729.

Dancer, P.N. & Pillar, N.W. 2001. Exploring in the Slyne Basin: a geophysical challenge. *The Petroleum Exploration of Ireland's Offshore Basins*, **188**, 209–222, https://doi.org/10.1144/GSL.SP.2001.188.01.12.

Dancer, P.N., Kenyon-Roberts, S.M., Downey, J.W., Baillie, J.M., Meadows, N.S. & Maguire, K. 2005. The Corrib gas field, offshore west of Ireland. *Geological Society, London, Petroleum Geology Conference series*, **6**, 1035–1046, https://doi.org/10.1144/0061035.

Deptuck, M.E. & Kendell, K.L. 2017. A Review of Mesozoic-Cenozoic Salt Tectonics Along the Scotian Margin, Eastern Canada. *In*: *Permo-Triassic Salt Provinces of Europe, North Africa and the Atlantic Margins*. 287–312., https://doi.org/10.1016/B978-0-12-809417-4.00014-8.

Dooley, T.P., Hudec, M.R., Pichel, L.M. & Jackson, M.P.A. 2018. The impact of base-salt relief on salt flow and suprasalt deformation patterns at the autochthonous, paraautochthonous and allochthonous level: insights from physical models. *Geological Society, London, Special Publications*, **476**, https://doi.org/10.1144/SP476.13.

Dooley, T.P., Jackson, M.P.A. & Hudec, M.R. 2013. Coeval extension and shortening above and below salt canopies on an uplifted, continental margin: Application to the northern Gulf of Mexico. *AAPG Bulletin*, **97**, 1737–1764, https://doi.org/10.1306/03271312072.

Doré, A.G., Lundin, E.R., Jensen, L.N., Birkeland, O., Eliassen, P.E. & Fichler, C. 1999. Principal tectonic events in the evolution of the northwest European Atlantic margin. *Petroleum Geology of Northwest Europe: Proceedings of the 5th Conference*, 41–61.

678 Doré, A.G., Corcoran, D. V. & Scotchman, I.C. 2002. Prediction of the hydrocarbon system
679 in exhumed basins, and application to the NW European margin. *Geological Society*
680 *Special Publication*, **196**, 401–429, https://doi.org/10.1144/GSL.SP.2002.196.01.21.

681 Duffy, O.B., Gawthorpe, R.L., Docherty, M. & Brocklehurst, S.H. 2013. Mobile evaporite
682 controls on the structural style and evolution of rift basins: Danish Central Graben,
683 North Sea. *Basin Research*, **25**, 310–330, https://doi.org/10.1111/bre.12000.

684 Dunford, G.M., Dancer, P.N. & Long, K.D. 2001. Hydrocarbon potential of the Kish Bank
685 Basin: Integration within a regional model for the Greater Irish Sea Basin. *Geological*
686 *Society Special Publication*, **188**, 135–154,
687 https://doi.org/10.1144/GSL.SP.2001.188.01.07.

688 Fyfe, L.-J.C., Schofield, N., Holford, S.P., Heafford, A. & Raine, R. 2020. Geology and
689 petroleum prospectivity of the Larne and Portpatrick basins, North Channel, offshore
690 SW Scotland and Northern Ireland. *Petroleum Geoscience*,
691 https://doi.org/10.1144/petgeo2019-134.

692 Hansen, T.H., Clausen, O.R. & Andresen, K.J. 2020. Thick- and thin-skinned basin inversion
693 in the Danish Central Graben, North Sea – the role of deep evaporites and basement
694 kinematics. *Solid Earth Discussions*, 1–39, https://doi.org/10.5194/se-2020-127.

695 Hassanpour, J., Yassaghi, A., Muñoz, J.A. and Jahani, S. 2021. Salt tectonics in a double
696 salt-source layer setting (Eastern Persian Gulf, Iran): Insights from interpretation of
697 seismic profiles and sequential cross-section restoration. *Basin Research*, **33**, 159–185,
698 https://doi.org/10.1111/bre.12459.

699 Hudec, M.R. & Jackson, M.P.A. 2007. Terra infirma: Understanding salt tectonics. *Earth-*
700 *Science Reviews*, **82**, 1–28, https://doi.org/10.1016/j.earscirev.2007.01.001.

701 Jackson, M.P.A. & Talbot, C.J. 1991. A glossary of salt tectonics. **91**. Bureau of Economic
702 Geology, University of Texas at Austin.

703 Jackson, M.P.A., Hudec, M.R. & Dooley, T.P. 2010. Some emerging concepts in salt
704 tectonics in the deepwater Gulf of Mexico: Intrusive plumes, canopy-margin thrusts,
705 minibasin triggers and allochthonous fragments. *Petroleum Geology Conference*
706 *Proceedings*, **7**, 899–912, https://doi.org/10.1144/0070899.

707 Jackson, M.P.A. and Hudec, M.R. 2017. Salt Pillows and Salt Anticlines. *In*: *Salt Tectonics*.
708 62–75., https://doi.org/10.1017/9781139003988.007.

709 Kimbell, G.S., Ritchie, J.D. & Henderson, A.F. 2010. Three-dimensional gravity and
710 magnetic modelling of the Irish sector of the NE Atlantic margin. *Tectonophysics*, **486**,
711 36–54, https://doi.org/10.1016/j.tecto.2010.02.007.

712 Knott, S.D., Burchell, M.T., Jolley, E.J. & Fraser, A.J. 1993. Mesozoic to Cenozoic plate
713 reconstructions of the North Atlantic and hydrocarbon plays of the Atlantic margins.
714 *Petroleum Geology of Northwest Europe: Proceedings of the 4th Conference*, 953–974,
715 https://doi.org/10.1144/0040953.

716 Kockel, F. 2003. Inversion structures in Central Europe - Expressions and reasons, an open
717 discussion. *Geologie en Mijnbouw/Netherlands Journal of Geosciences*, **82**, 367–382,
718 https://doi.org/10.1017/s0016774600020187.

719 Macaulay, E.A. 2017. A new approach to backstripping and sequential restoration in subsalt
720 sediments. *AAPG Bulletin*, **101**, 1385–1394, https://doi.org/10.1306/11291616122.

721 Magee, C., Jackson, C.A.L. & Schofield, N. 2014. Diachronous sub-volcanic intrusion along
722 deep-water margins: Insights from the Irish Rockall Basin. *Basin Research*, **26**, 85–105,
723 https://doi.org/10.1111/bre.12044.

724 Mark, N., Schofield, N., Gardiner, D., Holt, L., Grove, C., Watson, D., Alexander, A. & Poore,
725 H. 2019. Overthickening of sedimentary sequences by igneous intrusions. *Journal of*
726 *the Geological Society*, **176**, 46–60, https://doi.org/10.1144/jgs2018-112.

727 Merlin Energy Resources Consortium. 2020. The Standard Stratigraphic Nomenclature of
728 Offshore Ireland: An Integrated Lithostratigraphic, Biostratigraphic and Sequence
729 Stratigraphic Framework. Project Atlas. Petroleum Affairs Division, Department of the
730 Environment, Climate and Communications, Special Publication **1/21**.

731 Meyer, R., van Wijk, J. & Gernigon, L. 2007. The North Atlantic Igneous Province: A review
732 of models for its formation. *In*: *Special Paper 430: Plates, Plumes and Planetary*
733 *Processes*. 525–552., https://doi.org/10.1130/2007.2430(26).

734 Naylor, D. & Shannon, P.M. 2005. The structural framework of the Irish Atlantic Margin.
735 *Geological Society, London, Petroleum Geology Conference series*, **6**, 1009–1021,
736 https://doi.org/10.1144/0061009.

737 O'Reilly, B.M., Hauser, F., Jacob, A.W.B., Shannon, P.M., Makris, J. & Vogt, U. 1995. The
738 transition between the Erris and the Rockall basins: new evidence from wide-angle
739 seismic data. *Tectonophysics*, **241**, 143–163, https://doi.org/10.1016/0040-
740 1951(94)00166-7.

741 O'Sullivan, C.M., Childs, C.J., Saqab, M.M., Walsh, J.J. & Shannon, P.M. 2021. The
742 influence of multiple salt layers on rift-basin development; The Slyne and Erris basins,
743 offshore NW Ireland. *Basin Research*, 1–31, https://doi.org/10.1111/bre.12546.

744 Peel, F.J., Travis, C.J. & Hossack, J.R. 1995. Genetic structural provinces and salt tectonics
745 of the Cenozoic offshore US Gulf of Mexico: A preliminary analysis. *In*: *Salt Tectonics:*
746 *A Global Perspective*. 153–175.

747 Petersen, K., Clausen, O.R. & Korstgård, J.A. 1992. Evolution of a salt-related listric growth
748 fault near the d-1 well, block 5605, danish north sea: displacement history and salt
749 kinematics. *Journal of Structural Geology*, **14**, 565–577, https://doi.org/10.1016/0191-
750 8141(92)90157-R.

751 Quirk, D.G. & Pilcher, R.S. 2012. Flip-flop salt tectonics. *Geological Society Special*
752 *Publication*, **363**, 245–264, https://doi.org/10.1144/SP363.11.

753 Ramos, A., Fernández, O., Muñoz, J.A. & Terrinha, P. 2017. Impact of basin structure and
754 evaporite distribution on salt tectonics in the Algarve Basin, Southwest Iberian margin.
755 *Marine and Petroleum Geology*, **88**, 961–984,
756 https://doi.org/10.1016/j.marpetgeo.2017.09.028.

757 Rowan, M.G. 1993. A systematic technique for the sequential restoration of salt structures.
758 *Tectonophysics*, **228**, 331–348, https://doi.org/10.1016/0040-1951(93)90347-M.

759 Rowan, M.G. & Ratliff, R.A. 2012. Cross-section restoration of salt-related deformation: Best
760 practices and potential pitfalls. *Journal of Structural Geology*, **41**, 24–37,
761 https://doi.org/10.1016/j.jsg.2011.12.012.

762 Saqab, M.M., Childs, C., Walsh, J. & Delogkos, E. 2020. Multiphase deformation history of
763 the Porcupine Basin, offshore west Ireland. *Basin Research*, 1–22,
764 https://doi.org/10.1111/bre.12535.

765 Sclater, J.G. & Christie, P.A.F. 1980. Continental stretching: An explanation of the Post-Mid-
766 Cretaceous subsidence of the central North Sea Basin. *Journal of Geophysical*
767 *Research: Solid Earth*, **85**, 3711–3739, https://doi.org/10.1029/JB085iB07p03711.

768 Shannon, P.M. 1991. The development of Irish offshore sedimentary basins. *Journal of the*
769 *Geological Society*, **148**, 181–189, https://doi.org/10.1144/gsjgs.148.1.0181.

770 Shannon, P.M. 2018. Old challenges, new developments and new plays in Irish offshore
771 exploration. *Geological Society, London, Petroleum Geology Conference series*, **8**,
772 171–185, https://doi.org/10.1144/PGC8.12.

773 Snidero, M., Carrera, N., Mencos, J., Butillé, Granado, P., Tavani, S., Lopez-Mir, B., Sàbat,
774 F. & Muñoz, J.A. 2020. Diapir kinematics in a multi-layer salt system from the eastern
775 Persian Gulf. *Marine and Petroleum Geology*, **117**, 104402,
776 https://doi.org/10.1016/j.marpetgeo.2020.104402.

777 Statoil 2004. Well 19/11-1 & 1A Final Well Report. Statoil Exploration (Ireland) Ltd., compiled
778 by Hofsøy, R., Skagen, J., Mortensen, H. & Conroy, J.

779 Stoker, M.S., Stewart, M.A., Shannon, P.M., Bjerager, M., Nielsen, T., Blischke, A.,
780 Hjelstuen, B.O., Gaina, C., McDermott, K. & Ólavsdóttir. 2017. An overview of the
781 Upper Palaeozoic–Mesozoic stratigraphy of the NE Atlantic region. *Geological Society,*
782 *London, Special Publications*, **447**, 11–68, https://doi.org/10.1144/SP447.2.

783 Štolfová, K. & Shannon, P.M. 2009. Permo-Triassic development from Ireland to Norway:
784 basin architecture and regional controls. *Geological Journal*, **44**, 652–676,
785 https://doi.org/10.1002/gj.1187.

786 Shell 2011. Exploration Well IRE 18/20-G Wellbores 18/20-sb01 and 18/20-7 Final Well
787 Report Volume 2: Subsurface Section. Shell E&P Ireland Ltd., compiled by van
788 Koolwijk, M., Soek, H. & Stordal, T.

789 Stewart, S.A. & Coward, M.P. 1995. Synthesis of salt tectonics in the southern North Sea,
790 UK. *Marine and Petroleum Geology*, **12**, 457–475, https://doi.org/10.1016/0264-
791 8172(95)91502-G.

792 Stewart, S.A., Harvey, M.J., Otto, S.C. & Weston, P.J. 1996. Influence of salt on fault
793 geometry: Examples from the UK salt basins. *Geological Society Special Publication*,
794 **100**, 175–202, https://doi.org/10.1144/GSL.SP.1996.100.01.12.

795 Tari, G. & Jabour, H. 2013. Salt tectonics along the Atlantic margin of Morocco. *Geological*
796 *Society Special Publication*, **369**, 337–353, https://doi.org/10.1144/SP369.23.

Trueblood, S. & Morton, N. 1991. Comparative Sequence Stratigraphy and Structural Styles of the Slyne Trough and Hebrides Basin. *Journal of the Geological Society*, **148**, 197–201, https://doi.org/10.1144/gsjgs.148.1.0197.

Volozh, Y., Talbot, C. & Ismail-Zadeh, A. 2003. Salt structures and hydrocarbons in the Pricaspian basin. *American Association of Petroleum Geologists Bulletin*, **87**, 313–334, https://doi.org/10.1306/09060200896.

Walsh, A., Knag, G., Morris, M., Quinquis, H., Tricker, P., Bird, C. & Bower, S. 1999. Petroleum geology of the Irish Rockall Trough – a frontier challenge. *Petroleum Geology of Northwest Europe: Proceedings of the 5th Conference*, 433–444, https://doi.org/10.1144/0050433.

Walsh, J.J. & Watterson, J. 1991. Geometric and kinematic coherence and scale effects in normal fault systems. *Geological Society Special Publication*, **56**, 193–203, https://doi.org/10.1144/GSL.SP.1991.056.01.13.

Walsh, J.J., Bailey, W.R., Childs, C., Nicol, A. & Bonson, C.G. 2003. Formation of segmented normal faults: A 3-D perspective. *Journal of Structural Geology*, **25**, 1251–1262, https://doi.org/10.1016/S0191-8141(02)00161-X.

Withjack, M.O. & Callaway, S. 2000. Active normal faulting beneath a salt layer: An experimental study of deformation patterns in the cover sequence. *AAPG Bulletin*, **84**, 627–651.

Wilson, R.C.L., Hiscott, R.N., Willis, M.G. & Gradstein, F.M. 1989. The Lusitanian Basin of west-central Portugal: Mesozoic and Tertiary tectonic, stratigraphic, and subsidence history. *Extensional tectonics and stratigraphy of the North Atlantic margins*, 341–361.

Ziegler, P.A. & Dèzes, P. 2006. Crustal evolution of Western and Central Europe. *Geological Society, London, Memoirs*, **32**, 43–56, https://doi.org/10.1144/gsl.mem.2006.032.01.03.

Figure Captions

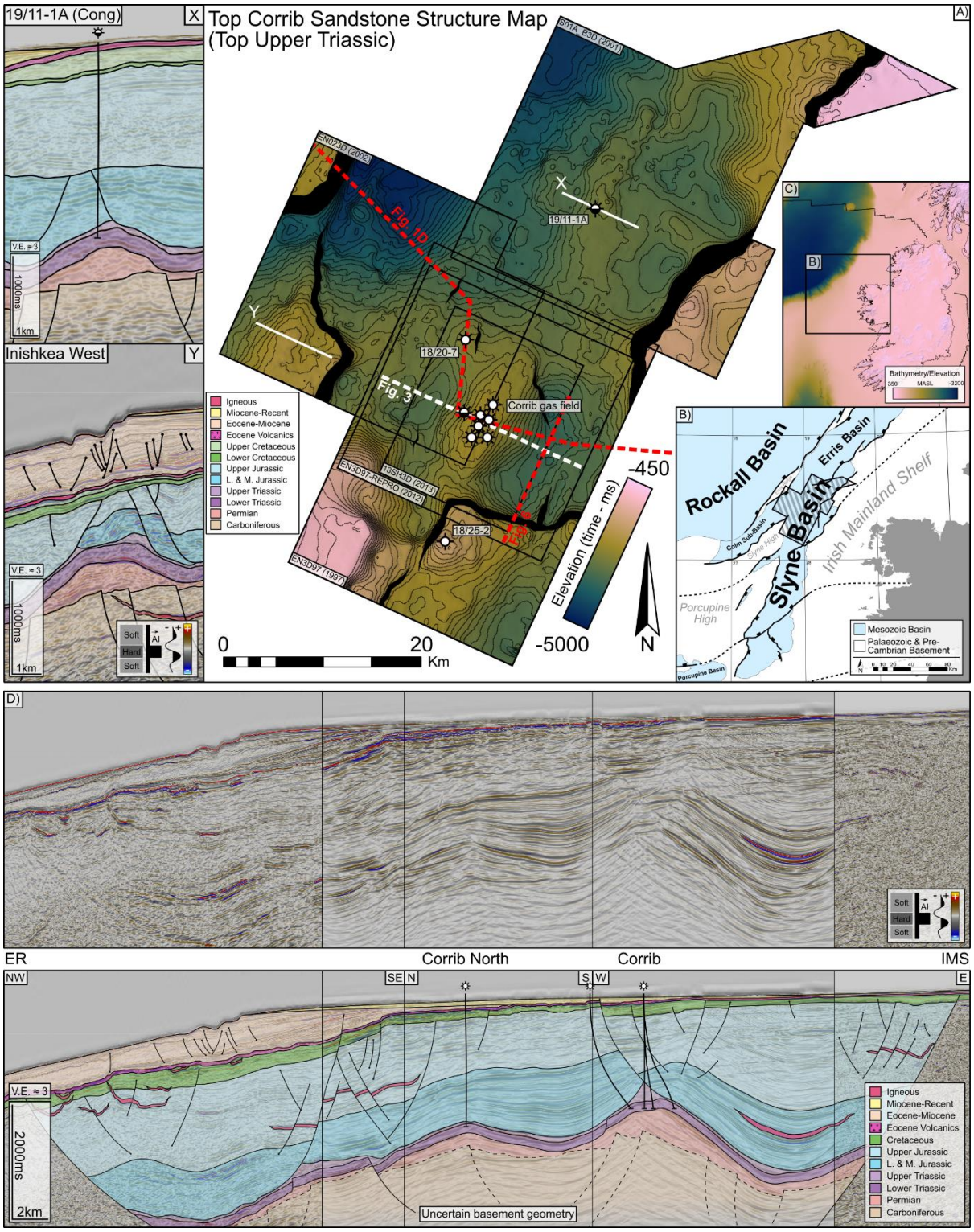

Figure 1: **A)** time structure map of the Lower Triassic Corrib Sandstone Formation in the Northern Slyne Sub-basin with outlines of 3D seismic volumes shown. Faults at Lower Triassic level shown with thick black polygons. Insets X and Y shows Corrib analogues in the Northern Slyne Sub-basin. **B)** Regional map showing the location of the study area and morphology of the Slyne Basin and neighbouring areas adapted from O'Sullivan et al. (2021). **C)** Regional bathymetry of the Irish Atlantic margin. **D)**

Regional arbitrary seismic line and accompanying geoseismic section showcasing the structural style of the Northern Slyne Sub-basin. Note the impact of Cenozoic thermal subsidence along the NW margin of the basin.

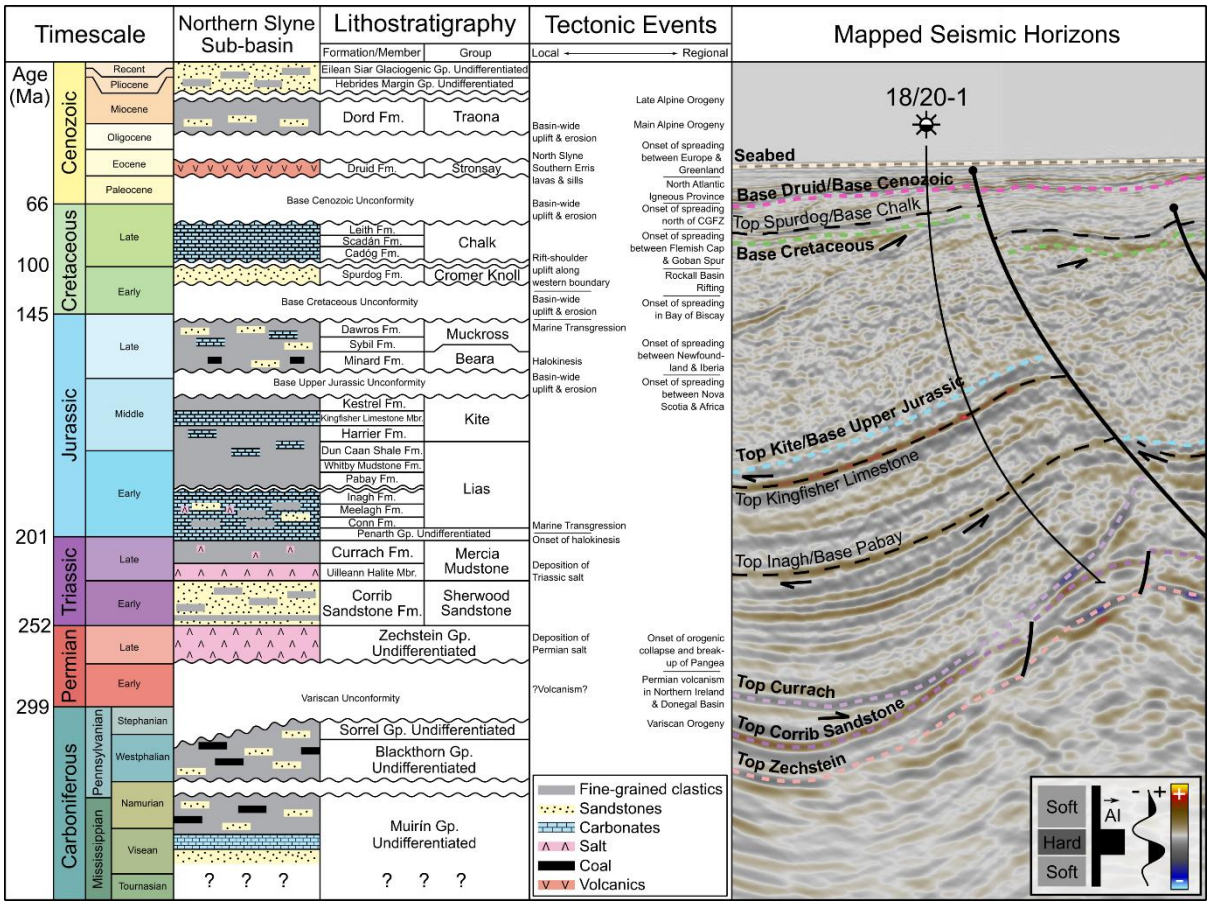

Figure 2: Simplified chronostratigraphic chart for the Northern Slyne Sub-basin showing the lithostratigraphic framework, local and regional tectonic events, and type seismic section through the Corrib gas field. Lithostratigraphic nomenclature adapted from Merlin Energy Resources Consortium (2020).

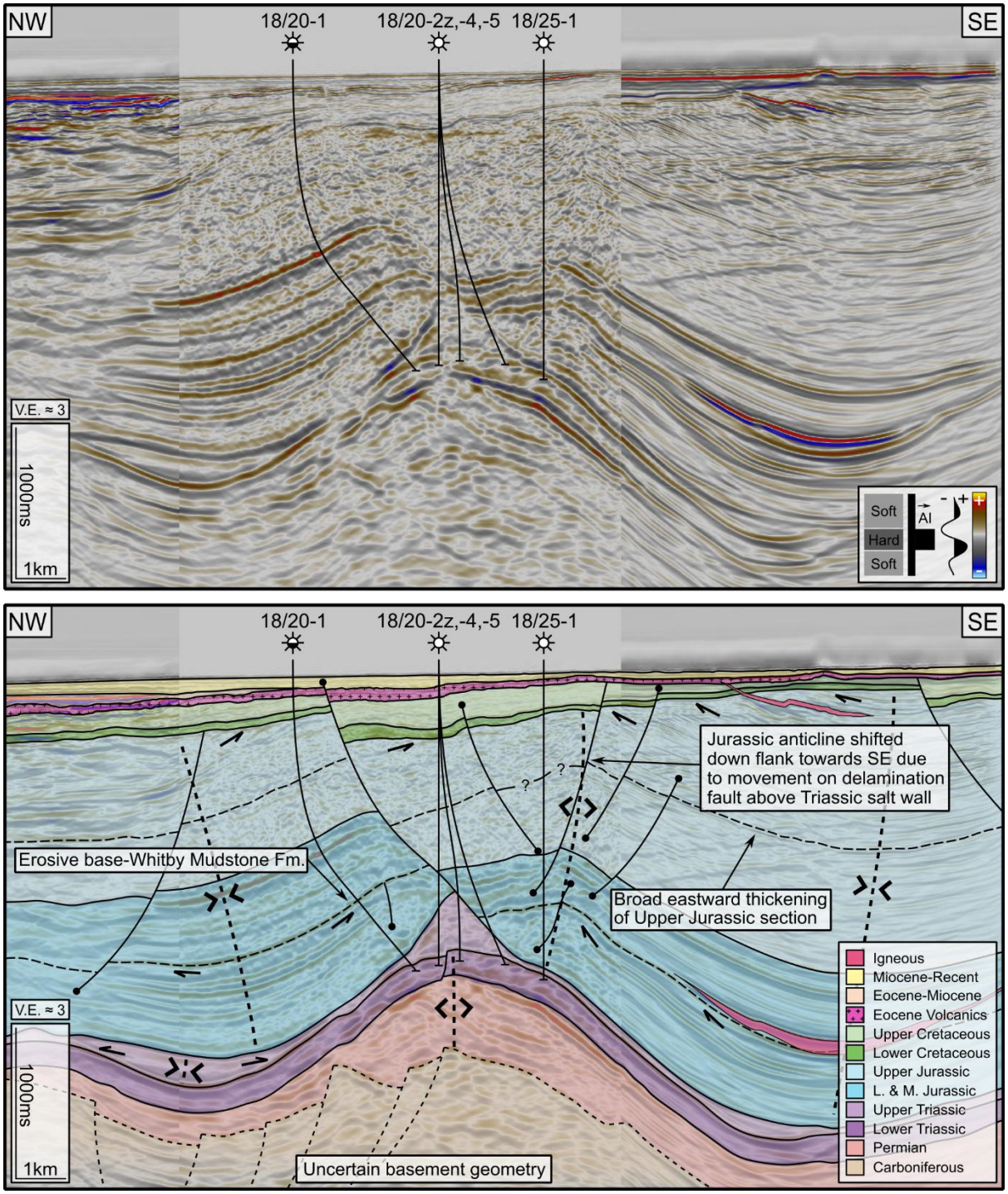

Figure 3: Composite section of the EN3D97-REPRO and 13SH3D seismic volumes and accompanying geoseismic interpretation across the Corrib gas field. See Figure 1 for seismic line location.

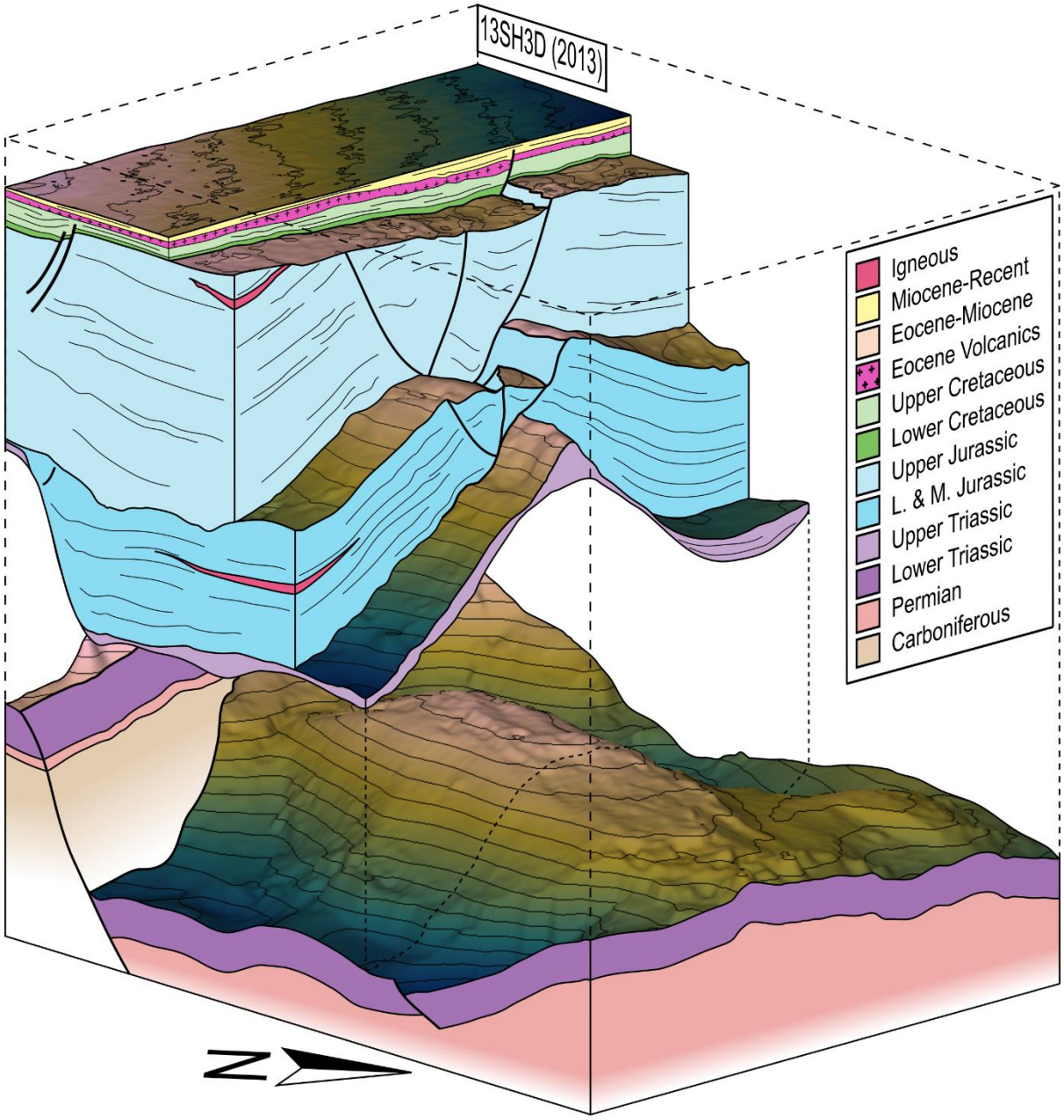

841

842 Figure 4: 3D block diagram illustrating the structural configuration of the Corrib gas field,
843 constructed from interpreted horizons within the 13SH3D seismic volume. The Upper
844 Triassic to Seabed section is elevated 1500 ms TWTT vertically.

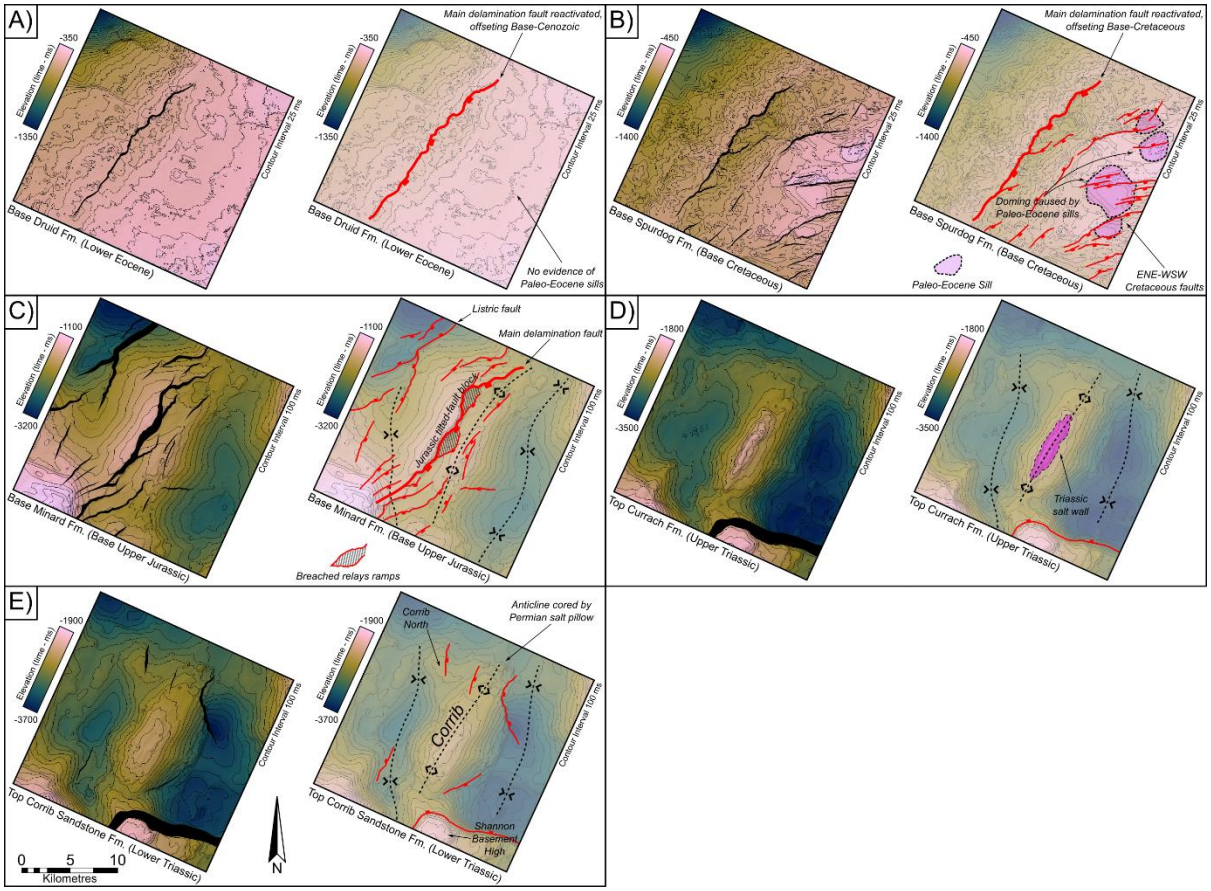

Figure 5: Time structure maps in ms TWTT created from the EN3D97-REPRO seismic volume illustrating the structural geometries observed at different stratigraphic levels. **A)** Base Druid Formation. **B)** Base Spurdog Formation. **C)** Base Minard Formation. **D)** Top Currach Formation. **E)** Top Corrib Sandstone Formation.

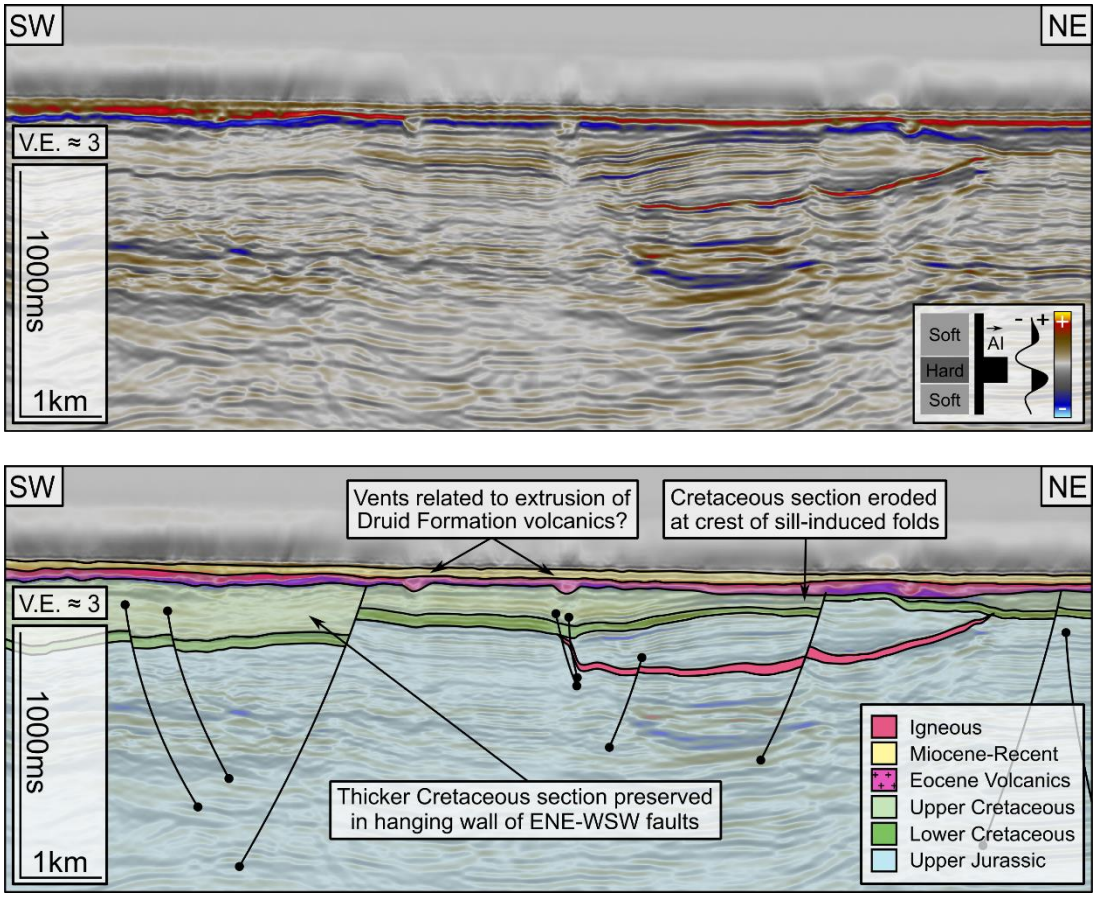

Figure 6: Seismic section and accompanying geoseismic interpretation of the shallow geology to the SE of the Corrib gas field, highlighting the impact of Cenozoic igneous activity on the Cretaceous geology. See Figure 1 for seismic line location.

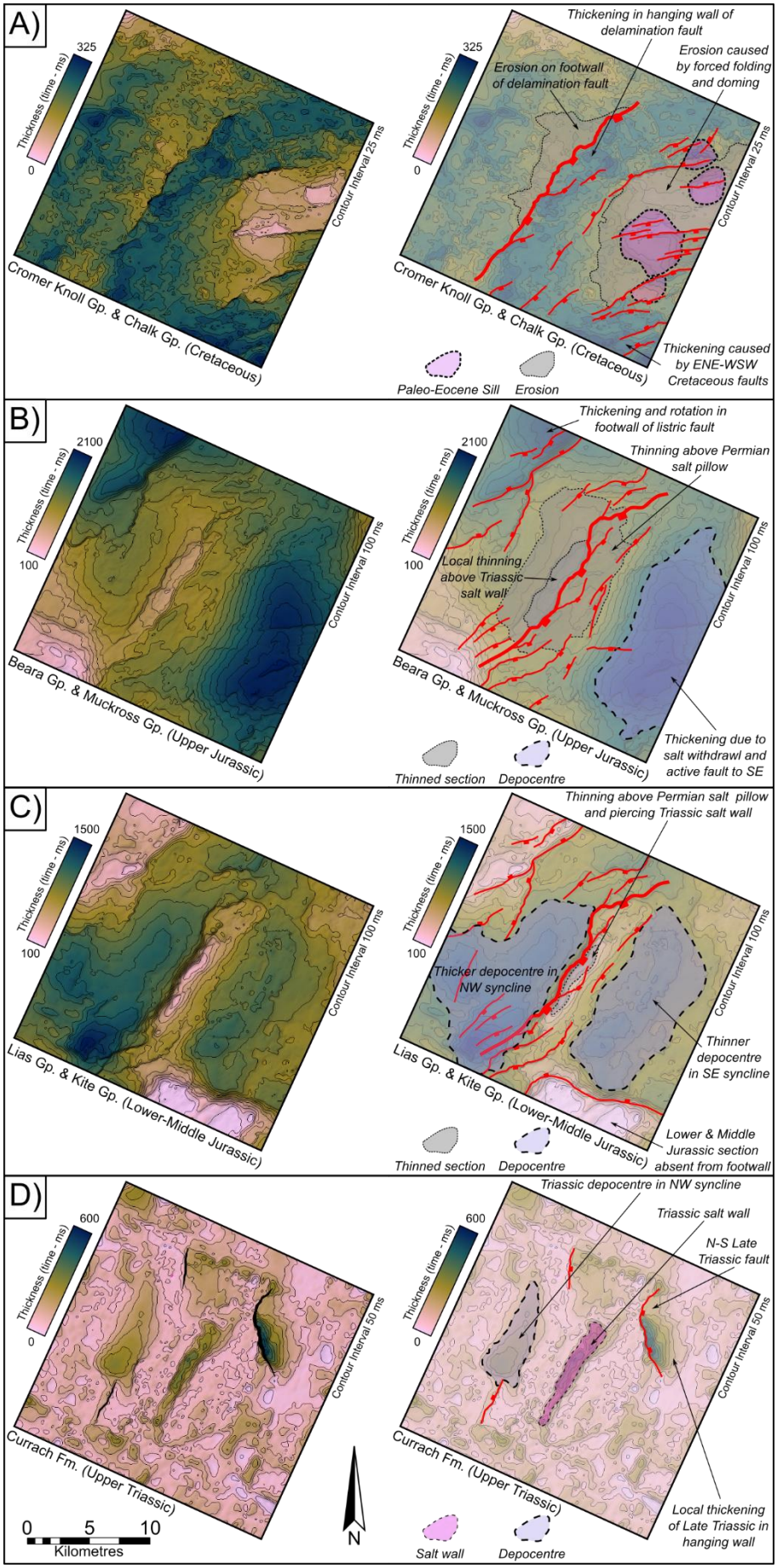
A)
325
Thickness (time - ms)
0
Contour Interval 25 ms
Cromer Knoll Gp. & Chalk Gp. (Cretaceous)
Thickening in hanging wall of delamination fault
Erosion caused by forced folding and doming
Erosion on footwall of delamination fault
Thickening caused by ENE-WSW Cretaceous faults
Paleo-Eocene Sill
Erosion
B)
2100
100
Contour Interval 100 ms
Beara Gp. & Muckross Gp. (Upper Jurassic)
Thickening and rotation in footwall of listric fault
Thinning above Permian salt pillow
Local thinning above Triassic salt wall
Thickening due to salt withdrawl and active fault to SE
Thinned section
Depocentre
C)
1500
Thinning above Permian salt pillow and piercing Triassic salt wall
Thicker depocentre in NW syncline
Thinner depocentre in SE syncline
Lias Gp. & Kite Gp. (Lower-Middle Jurassic)
Lower & Middle Jurassic section absent from footwall
D)
600
Contour Interval 50 ms
Currach Fm. (Upper Triassic)
Triassic depocentre in NW syncline
Triassic salt wall
N-S Late Triassic fault
Local thickening of Late Triassic in hanging wall
0 5 10
Kilometres
N
Salt wall

Figure 7: Time thickness (isochron) maps in ms TWTT created from horizons presented in Figure 5. **A)** Cromer Knoll & Chalk groups. **B)** Beara and Muckross groups. **C)** Lias and Kite groups. **D)** Currach Formation.

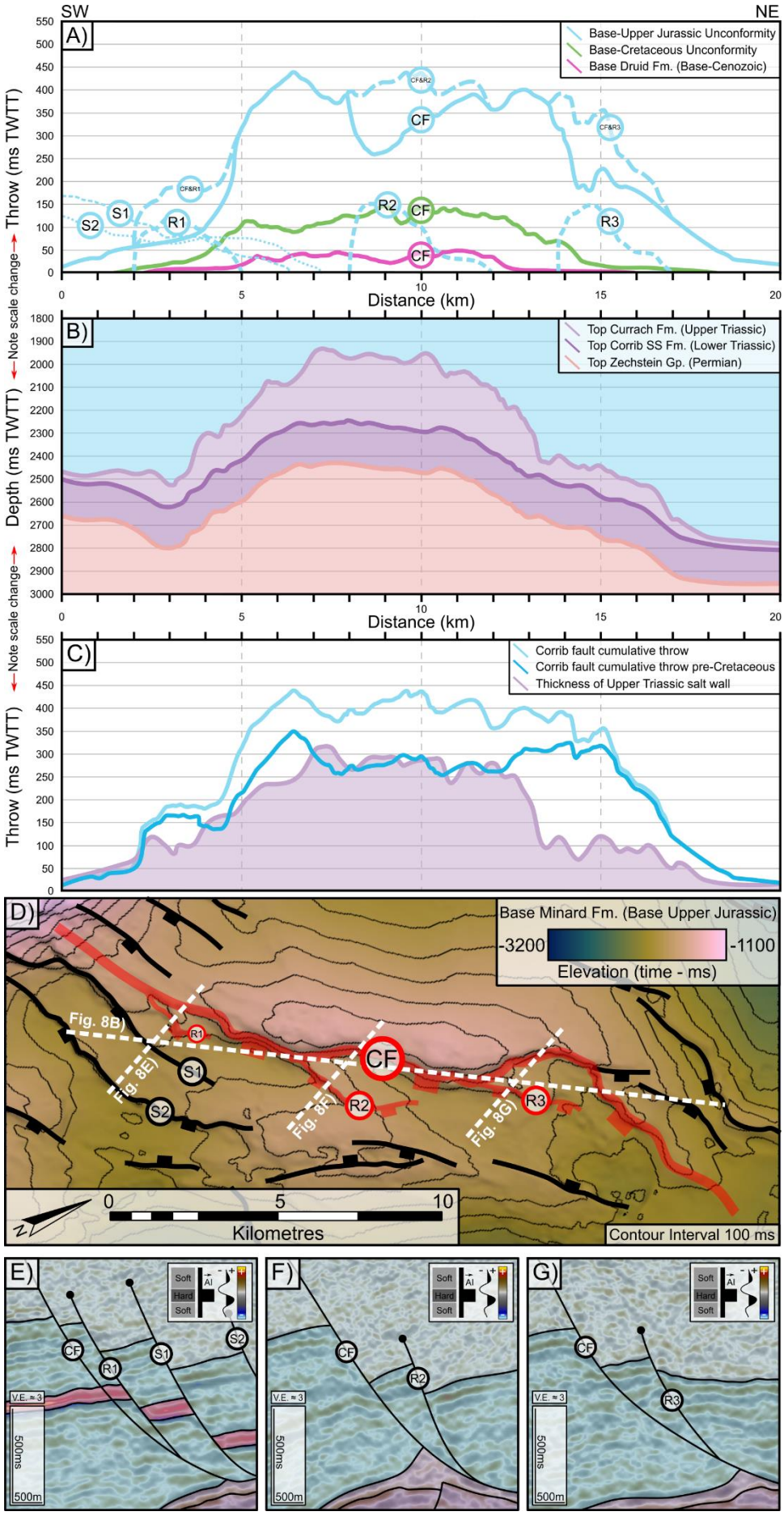
SW
NE
A)
Base-Upper Jurassic Unconformity
Base-Cretaceous Unconformity
Base Druid Fm. (Base-Cenozoic)
Throw (ms TWTT)
Note scale change
CF&R2
CF
CF&R3
CF&R1
S1
S2
R1
R2
R3
Distance (km)
B)
Top Currach Fm. (Upper Triassic)
Top Corrib SS Fm. (Lower Triassic)
Top Zechstein Gp. (Permian)
Depth (ms TWTT)
Distance (km)
C)
Corrib fault cumulative throw
Corrib fault cumulative throw pre-Cretaceous
Thickness of Upper Triassic salt wall
Throw (ms TWTT)
D)
Base Minard Fm. (Base Upper Jurassic)
-3200
-1100
Elevation (time - ms)
Fig. 8B)
Fig. 8E)
Fig. 8F)
Fig. 8G)
Kilometres
Contour Interval 100 ms
E)
F)
G)
Soft
Hard
Soft
AI
V.E. ≈ 3
500ms
500m

Figure 8: **A)** Throw-distance (T-x) plot displaying the along-strike throw of the Corrib fault system for prominent syn-rift and post-rift horizons. **Abbreviations:** CF – Corrib Fault; R1-3 – Hanging-wall splays; S1-2 – Additional faults **B)** Simplified cross-section through the time-structure maps of the Top Currach and Corrib Sandstone formations and Zechstein Group. For cross-section location see Figure 7D). **C)** Throw-distance (T-x) plot displaying the along-strike throw of the Corrib fault for the Base Upper Jurassic Unconformity alongside the backstripped pre-Cretaceous throw, and the thickness of the Upper Triassic salt wall. **D)** Time structure map of the Base Minard Formation adjacent to the delamination fault system, highlighting the fault planes displayed in Figure 7A). **E-G)** Geoseismic sections along the Corrib fault showing fault linkage geometries.

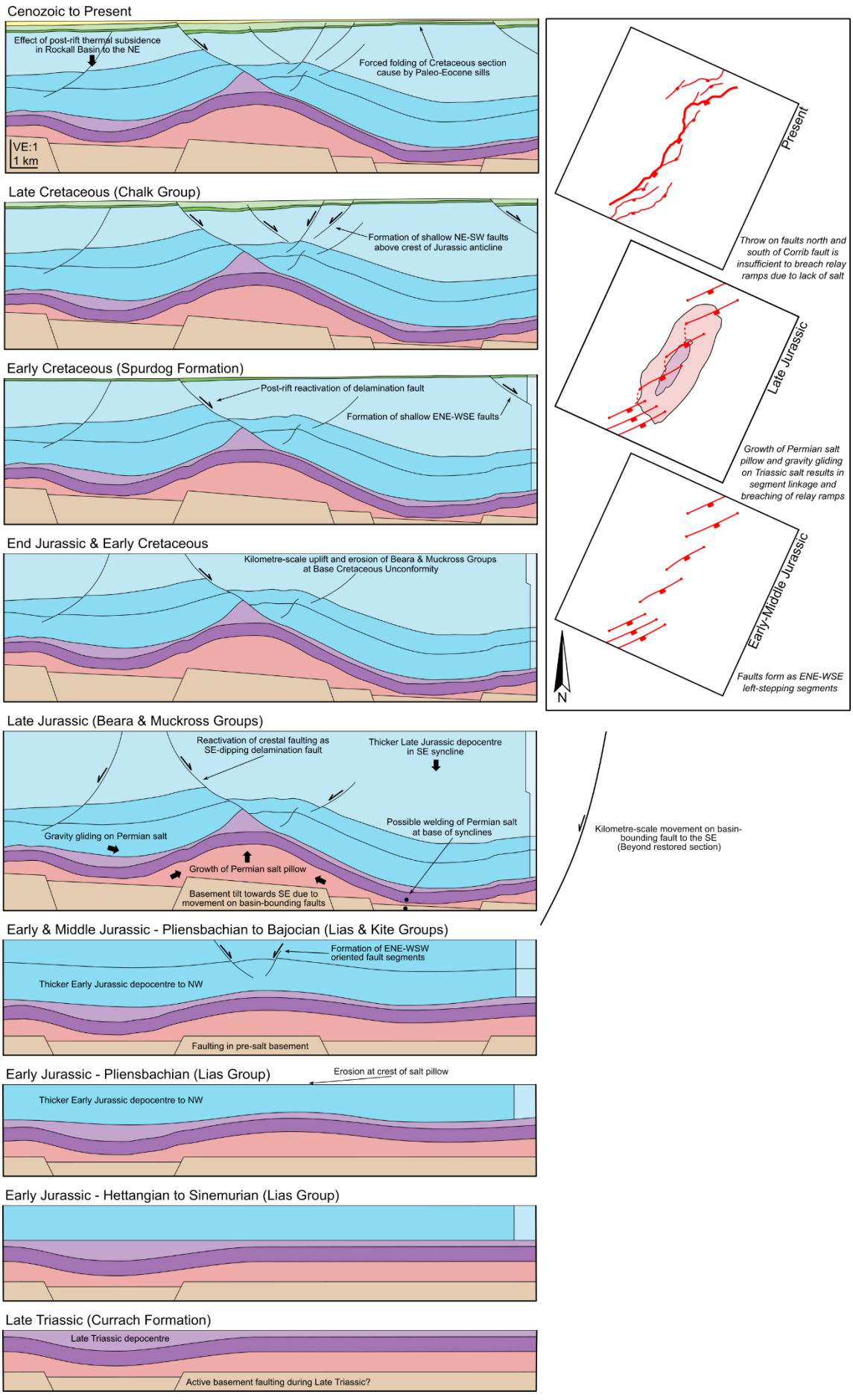
Cenozoic to Present
Effect of post-rift thermal subsidence in Rockall Basin to the NE
Forced folding of Cretaceous section cause by Paleo-Eocene sills
VE:1
1 km
Late Cretaceous (Chalk Group)
Formation of shallow NE-SW faults above crest of Jurassic anticline
Early Cretaceous (Spurdog Formation)
Post-rift reactivation of delamination fault
Formation of shallow ENE-WSE faults
End Jurassic & Early Cretaceous
Kilometre-scale uplift and erosion of Beara & Muckross Groups at Base Cretaceous Unconformity
Late Jurassic (Beara & Muckross Groups)
Reactivation of crestal faulting as SE-dipping delamination fault
Thicker Late Jurassic depocentre in SE syncline
Possible welding of Permian salt at base of synclines
Gravity gliding on Permian salt
Growth of Permian salt pillow
Basement tilt towards SE due to movement on basin-bounding faults
Kilometre-scale movement on basin-bounding fault to the SE (Beyond restored section)
Early & Middle Jurassic - Pliensbachian to Bajocian (Lias & Kite Groups)
Formation of ENE-WSW oriented fault segments
Thicker Early Jurassic depocentre to NW
Faulting in pre-salt basement
Early Jurassic - Pliensbachian (Lias Group)
Erosion at crest of salt pillow
Thicker Early Jurassic depocentre to NW
Early Jurassic - Hettangian to Sinemurian (Lias Group)
Late Triassic (Currach Formation)
Late Triassic depocentre
Active basement faulting during Late Triassic?
Present
Throw on faults north and south of Corrib fault is insufficient to breach relay ramps due to lack of salt
Late Jurassic
Growth of Permian salt pillow and gravity gliding on Triassic salt results in segment linkage and breaching of relay ramps
Early-Middle Jurassic
Faults form as ENE-WSE left-stepping segments
N

Figure 9: Sequential structural restoration of the interpreted seismic section presented in Figure 3 with no vertical exaggeration. Due to uncertainty in the actual geometry of the sub-salt basement in the Northern Slyne Sub-basin, a schematic basement is included to suggest potential drivers for halokinesis based on interpretation of basement structures elsewhere in the Slyne Basin (e.g. O'Sullivan et al., 2021). Inset: schematic evolution of the fault system in the supra-salt Jurassic section.

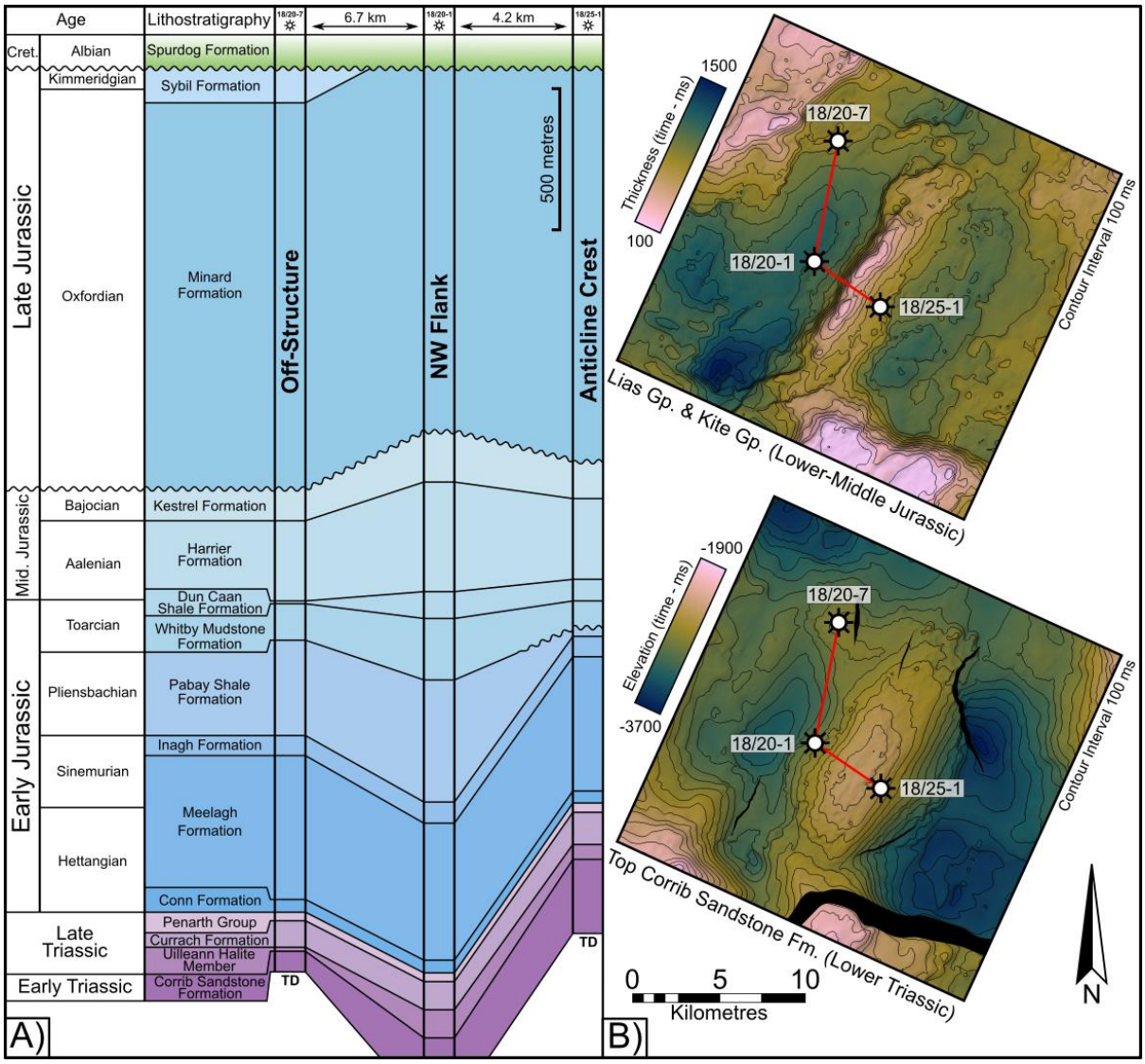

Figure 10: **A)** Well correlation through the three wells which penetrate a complete Jurassic section within the EN3D97-REPRO seismic volume. The Base-Cretaceous Unconformity is the datum. The 18/20-7 well is representative of the Jurassic section off-structure, while the 18/20-1 is representative of the Early Jurassic depocenter on the NW flank. The 18/25-1 well showcases the Early-Middle Jurassic crest of the salt-cored fold, before the delamination fault downthrows this crest onto the SE flank of the structure during the Late Jurassic. Notice the isopachous nature of the Conn, Meelagh and Inagh formations. **B)** Time thickness (isochron) map of the Lias and Kite groups and a time structure map of the Corrib Sandstone Formation, both in ms TWTT, showing the location of the well correlation.